https://doi.org/10.1070/RCR5031

Ionic liquid glasses: properties and applications

Mikhail Yu. Ivanov,[a] Nikolay V. Surovtsev,[b] Matvey V. Fedin [a]

[a] *International Tomography Center, Siberian Branch of the Russian Academy of Sciences, ul. Institutskaya 3a, 630090 Novosibirsk, Russian Federation*
[b] *Institute of Automation and Electrometry, Siberian Branch of the Russian Academy of Sciences, prosp. Akademika Koptyuga 1, 630090 Novosibirsk, Russian Federation*

Ionic liquids (ILs) are considered as an alternative to conventional organic solvents used in industry, and the distinctive physical and chemical properties of these substances are being actively investigated. Ionic liquids can be applied in a number of areas, including polymerization reactions, catalysis and biomedicine. Although the overwhelming majority of studies are focused on the liquid state of ILs, an understanding of their properties in a glassy state can stimulate innovations in organic synthesis, energy storage and cryopreservation. This review aims at a systematic description of the properties and applications of ILs in the glassy state, which has not been published previously and appears relevant and demanded by the scientific community.
The bibliography includes 286 references.

Contents

1. Introduction 1
2. General overview of physicochemical properties of glasses 2
3. Glass transition temperature of ionic liquids 5
3.1. Influence of cation(anion) structure on T_g 5
3.2. Glass transition temperature of IL under external pressure 6
3.3. Correlation of T_g with IL molar volume 7
3.4. Glass transition temperature of nanoconfined ILs 7
3.5. Glass transition temperature for IL mixtures 8
4. Heterogeneous structure of ionic liquid glasses 8
4.1. Neutron and X-ray scattering 8
4.2. Dielectric spectroscopy 9
4.3. Solid-state NMR 10
4.4. Temperature-modulated DSC 10
4.5. Electron paramagnetic resonance 11
4.6. Molecular dynamics 12
5. Pharmaceutical applications 12
6. Cryopreservation applications 13
7. Polymerization and energy applications 14
7.1. Plasticizer effect 14
7.2. Solid-state electrolytes 15
8. Conclusion 16
9. List of acronyms and designations 16
10. References 16

1. Introduction

Ionic liquids are a promising class of substances that find an increasing number of applications in various fields of science and industry.[1–3] A number of unique physical and chemical properties of ILs allow them to be used as new low-toxicity solvents in green chemistry,[4] as drug delivery agents in biomedicine[5] and as components of new functional nanomaterials.[6] Interest in the properties and applications of ILs is evident since, despite more than thirty years of active research, many articles on this class of compounds continue to be published in top-ranked scientific journals.[5,7–11]

By definition, ILs have a melting temperature below 100 °C, have promising properties such as high thermal stability, a low vapour pressure, a wide electrochemical window and inspiring solubilizing characteristics.[12,13]

Nowadays most of the studies focus on the properties and applications of ILs in the liquid state. However, the past decade showed a new trend of increasing interest in solid ILs, particularly in the crystalline[14–17] and glassy (or amorphous) states.[6,18–20] Speaking of IL crystals, a number of exhaustive reviews[15,17,21] have been published, describing the fundamentals and main applications of IL crystals as anisotropic ion-conducting materials,[22,23] electrolytes in dye-sensitized solar cells,[24,25] organized media for synthesis[26,27] and photoluminescent materials.[28,29] Meanwhile,

M.Yu.Ivanov. PhD in Physical and Mathematical sciences, Researcher in in the International Tomography Center of the SBRAS.
E-mail: michael.ivanov@tomo.nsc.ru
Current research interests: application of EPR techniques in materials science, study of heterogeneities in ionic liquids glasses, triplet systems with π-conjugation, electron-acceptor dyads, EPR instrumentation, microwave engineering.
N.V.Surovtsev. Corresponding member of RAS, Doctor of Physical and Mathematical sciences, Professor of RAS, Head of the Laboratory of Condensed Matter Spectroscopy at the Institute of Automation and Electrometry of the SBRAS.
E-mail: snv@iae.nsk.su
Current research interests: condensed matter spectroscopy, the use of Raman scattering of light in solving urgent problems of physics of disordered media and biophysics.
M.V.Fedin. Doctor of Physical and Mathematical sciences, Professor of RAS, Head of the Laboratory of EPR spectroscopy in the International Tomography Center of the SBRAS.
E-mail: mfedin@tomo.nsc.ru
Current research interests: methodology and applications of EPR to biological systems and materials science.

Received 30 June 2021

© 2022 Uspekhi Khimii, ZIOC RAS, Russian Academy of Sciences and IOP Publishing Limited

no reviews describing the main characteristics and applications of IL glasses are available. This probably stems from a supportive role of glassy state properties in revealing the key characteristics of the corresponding liquid or crystalline states. The current review, in particular, collects the hot-topic examples, where glassy state properties of ILs create the basis for their applications in other states. It is well known that catalytic applications of ILs are widely developed, driving the interest in this type of matter.[4, 30–33] Applications of ILs in catalysis mainly rely on structural heterogeneity that leads to a number of their specific properties, such as the ability to dissolve both polar and non-polar compounds, the ability for amphiphilic self-organization, and nonlinear effects upon increasing the alkyl chain length.[88] Importantly, the glassy state provides a very convenient way to study these intriguing and key relationships between the property and the heterogeneous structure on the molecular scale (see Section 4).[34–39] Therefore, the narrative of this review is focused on the effects that the heterogeneous structure of ILs imposes on glass properties, as is revealed by many independent experimental approaches.[40–43] The growing interest in biological and pharmaceutical applications of ILs[55] emphasizes the importance of understanding the amorphous states of these materials, which again are tightly interconnected with the corresponding glassy states (see Section 5). In terms of biological applications of ILs, cryopreservation attracts a significant attention: the versatile properties of IL glasses can be widely employed, thus allowing them to function as commonly used cryoprotectants (see Section 6). The development of IL-based agents for functional polymers is another important field of the rapidly growing plastics industry:[44] ionic liquids behave as great plasticizers and sufficiently improve mechanical performance of such commonly used polymers as poly(methyl methacrylate) (PMMA)[45–47] and poly(vinyl chloride) (PVC)[48] (see Section 7.1). Considering the importance of IL-based materials in electrochemical applications,[2, 29] the knowledge of the glass transition temperature (T_g) and fragility[50] is a cornerstone of successful design of solid electrolytes. In fact, glass state properties are generally crucial for such applications of ILs, even if they are used at ambient temperature. A number of developed polymer gels[51] and ionogels[52–54] are also extensively used as solid electrolytes (see Section 7.2).[55, 56]

It is important to note that we address only those ILs, which are liquid at ambient temperature and therefore are called *room-temperature* ILs. Compounds with a melting point higher than 373 K are often referred to as *molten salts,* and they are not covered in this review.

Finally, we would like to introduce the term '*ionic liquid glasses*', which is used throughout this review, but has not yet become commonly accepted. Speaking of 'IL glasses', we refer specifically to a glassy state (typically formed at low temperatures) of room-temperature ionic liquids. There is another well-established term '*ionic glasses*', thoroughly employed by Angell[57] and other scientists. However, this term is more general and might refer also to many inorganic substances beyond ionic liquids. Certainly, the fundamental physicochemical properties of '*ionic glasses*' and '*ionic liquid glasses*', as well as experimental approaches used in their studies, are strongly correlated. However, from our point of view, the abundant diversity of IL structures encompassing nontrivial combinations of organic and inorganic moieties makes the distinguishing of '*IL glasses*' from '*ionic glasses*' reasonable and well-justified; moreover, the specific studies on IL glasses — the glassy states of ILs — are growing in number in modern science (Fig. 1).

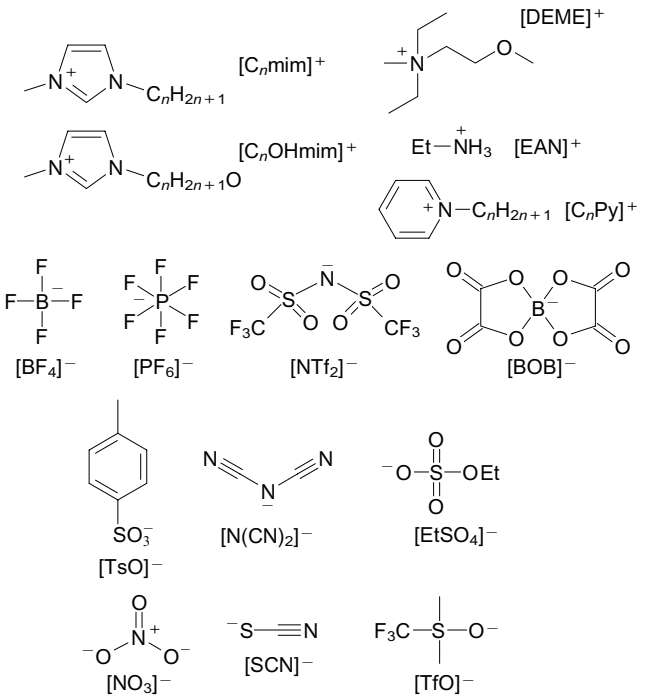


Figure 1. Ionic liquid cations and anions most frequently addressed in this review.

2. General overview of physicochemical properties of glasses

This Section introduces some basic physicochemical properties of glasses, whereas the detailed structure–property relationships for ILs will be discussed in the rest of this review.

The modern definition of the glassy state given in 2017 claims that 'glass is a non-equilibrium, non-crystalline state of matter that appears solid on a short time scale but continuously relaxes towards the liquid state'.[58] Glasses have no long-range(periodic) atomic order; the translational and orientational motions of basic structural units are suppressed, while the rotational motions of specific local moieties can sometimes be observed. On a short-time scale (< 100 s at temperatures near the glass transition temperature, T_g), the glassy state possesses mechanical properties resembling the solid state, but the absence of a long-range order and a finite relaxation time make it similar to a supercooled liquid state in some aspects. It is often believed that in the infinitely longtime limit, the glass tends to transform to a thermodynamically stable state, *i.e.*, to the crystalline state. Glassy materials with an age of about of 20 million years are known in nature.[59,60]

Below we briefly introduce the most common and simple terms and concepts relevant for the glassy state in general and applicable for the majority of IL glasses in particular.

The fragility index m (also called the steepness index) characterizes the degree of deviation from the Arrhenius law for the temperature dependences of the main physical parameters (viscosity, α-relaxation, ion diffusion, *etc.*). The m index essentially represents the activation energy at the

glass transition temperature in units of $k_B T_g$ (k_B is the Boltzmann constant). In term of structural relaxation time τ_α, m can be represented as:[61]

$$m = \left.\frac{d\log\tau_\alpha}{d(T_g/T)}\right|_{T\,=\,T_g} \quad (1)$$

The fragility index defined by Eq. (1) describes the temperature dependence of the relaxation time near the glass transition temperature T_g. In a certain sense, it reflects the jamming effect, leading to an increase in the effective activation barrier with temperature. In these terms, the fragility index can be associated with the freezing of degrees of freedom during cooling near T_g. Besides, the freezing(releasing) of degrees of freedom has a counterpart in specific heat measured by differential scanning calorimetry (DSC).

Indeed, it was found that the fragility index m correlates with DSC curve parameters.[11] The fragility index m was found to be inversely proportional to the heat capacity step in the $C_P(T)$ plot measured by DSC, as will be described in the following Section. Thermodynamic fragility can be evaluated *via* an empirical correlation based on a large amount of experimental calorimetric data for typical glass-forming substances:[62]

$$m = \frac{56 T_g \Delta C_p(T_g)}{\Delta H_m} \quad (2)$$

where ΔH_m is the enthalpy of melting, T_g is the glass transition temperature and $\Delta C_p(T_g)$ is the jump in the heat capacity at T_g. In the case of ionic liquids, the value of $\Delta C_p(T_g)$ is determined mainly by configurational dynamics of the cation alkyl chain and is roughly independent of the structure of anions.[63–65] The fragility index is widely used to compare and scale the viscous flow behaviour of glass-forming liquids, which is crucial for energy applications of ionic liquids.[50] It is also used to identify the structural stability of glass formers; the fragility index helps to classify and arrange all glasses from *strong* ($m \sim 20$) to *fragile* ($m \sim 100$) ones. Strong glasses follow an Arrhenius behaviour and are often represented by inorganic glass-formers with tetrahedral geometry of intramolecular bonds. Strong glass-formers are believed to have higher fluctuations in elastic properties on the nanometre scale, but they also demonstrate less pronounced dynamic heterogeneities in the vicinity of T_g. Fragile glasses, conversely, are characterized by a very rapid decrease in the viscosity near T_g and smaller changes at higher temperatures. Fragile liquids exhibit more cooperative glass transition; in addition, they are often structurally less stable than the strong glasses.[66,67] Strong and fragile glass-formers have different ratios between relaxation and vibrational motions near T_g, which is closely related to the temperature dependence of viscosity and conductivity of these compounds.[68] Figure 2 shows the data on the fragility index (m) *vs* T_g for a wide range of IL and non-IL glass-formers.

Also, Fig. 2 illustrates the place of ILs among a wide variety of common glass-formers, revealing that the majority of ILs span the range from medium-strength to very fragile glass-formers with T_g in the range of 180–250 K. Despite the illustrative character of such plots, some useful correlations between m, T_g and the energy parameters were obtained.[71]

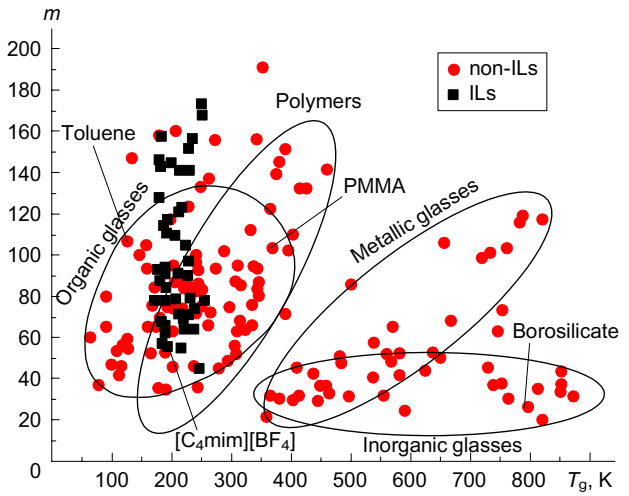


Figure 2. Fragility and T_g data for IL and non-IL glass-formers. The Figure was prepared by the authors using the data from the studies.[18,50,69–71]

Probably most of the known models that describe the relaxation as well as the viscosity (η) and the conductivity (σ) in glasses are reviewed in the classical work by Angell *et al.*[72] The relaxation time (τ) and the viscosity are extremely sensitive to the temperature in the vicinity of T_g, and the Vogel–Fulcher–Tammann (VFT) equation is mostly used to describe the temperature dependence of the viscosity/relaxation time:[73,74]

$$\tau = \tau_0 \exp\frac{B}{T - T_\infty} \quad (3)$$

where τ_0, B and T_∞ are the constants, the physical meaning of which differs in various theoretical interpretations. In general, $T_\infty = 0$ results in the common Arrhenius law with $B = E/k_B$, where E is the activation energy barrier and k_B is the Boltzmann constant. In the case of $T_\infty > 0$, the temperature dependence is non-Arrhenius, and the relaxation time is predicted to become infinite at T_∞. The VFT expression is only an approximation, since the activation energy cannot reach the infinity at a finite temperature.[75]

The VFT relation is often used to analyze the temperature dependence of the conductivity for direct current (σ_{DC}) in glass-forming ILs near T_g and can be rewritten in the modified form:

$$\sigma_{DC} = \sigma_0 \exp\left(-\frac{DT_{VF}}{T - T_{VF}}\right) \quad (4)$$

where σ_0 reflects the conductivity at high temperature limit. The adjustable parameter T_{VF} is usually lower than T_g; D is the so-called strength parameter, which is also used in the classification scheme for glass-formers to distinguish between strong and fragile glasses.[76] The parameters D and m are interconnected by the relation $m = 16 + 590/D$.[69] Figure 3 demonstrates how the T_g and m (or D) parameters influence $\sigma_{DC}(T)$, where the curves for four hypothetical ILs (depicted as A–D) with different T_g and m values are shown.[50]

Substances A and B have identical high fragilities ($m = 150$ or $D = 4.4$) and demonstrate the effect of different T_g. Glasses A and C (or B and D) have identical T_g but

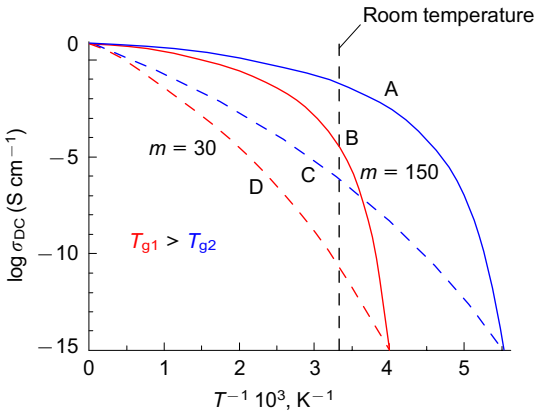


Figure 3. Temperature dependence of the conductivity for ILs with different T_g and m values. The Figure was prepared by the authors using the data from the study.[50]

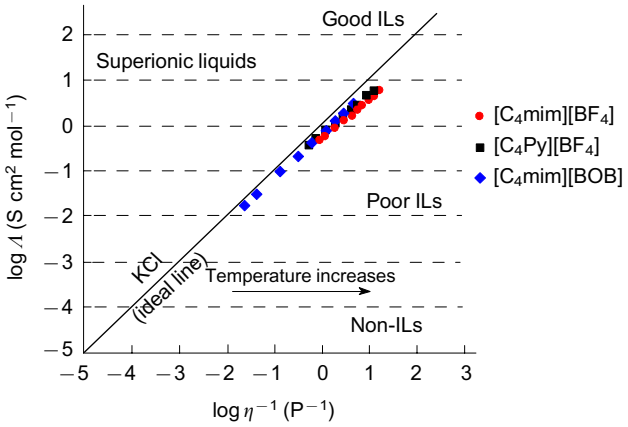


Figure 4. Relationship between the equivalent conductivity and viscosity (Walden plot) for some ILs. The Figure was prepared by the authors using the data from the study.[82]

different fragilities (glasses C and D have $m = 30$ and $D = 42$), thus demonstrating the significant influence of fragility on the conductivity. It is important to note the effect of conductivity enhancement for the sample with a small T_g value. Note that Fig. 3 is illustrative: in particular, the infinite temperature corresponding to the zero x axis value is never reached in real experiments due to sample decomposition.

However, the characterization of ionic conductivity in the vicinity of T_g should be considered carefully because the diffusion coefficient sufficiently deviates from the classical Stokes–Einstein relationship: $D\tau_\alpha = \text{const}$ — this is the so-called decoupling of translational diffusion from structural relaxation. Such behaviour is typical even of conventional glass-forming liquids, *e.g.*, *ortho*-terphenyl [77] or trinaphthylbenzene,[78] but the decoupling mechanism is still debatable. Some studies show that the diffusion decoupling correlates with fragility.[79, 80] For example, Griffin *et al.*[81] demonstrated that the decoupling strength in IL [C$_4$mim][NTf$_2$] is considerably lower compared to non-IL glass-forming substances with similar fragility ($m \approx 97$), and a more pronounced correlation was found for the decoupling with the viscosity of the material rather than with m.

It is important that the T_g and the fragility values are used to determine the liquid fluidity and conductivity at ambient temperature. Therefore, the glassy state is strongly related to viscosity/conductivity phenomena, and the relationship between the conductivity and the viscosity at different temperatures should also be described. Historically, the Walden rule was explicit for strong electrolytes, where the fluidity (inverse viscosity) and the conductivity change with temperature at the same rate.[82] The Walden rule is used to identify the transport property relationship and to estimate the ionicity of ILs, it can be written as

$$\Lambda\eta = \text{const} \qquad (4)$$

where Λ is the equivalent conductivity (*i.e.*, the conductivity normalized to the volume that contains one Faraday of positive ions, $\Lambda = \sigma V$) and η is the viscosity. The Walden plot approach is especially suitable for ILs. It serves to emphasize the relationship between the ionic conductivity and vapour pressure. The rule provides a basis for a very useful classification of ILs represented by the Walden plot (4).[82]

It is common to use data for dilute aqueous KCl solution as a reference for the ideal Walden line because this solution completely dissociates and has ions of equal mobility (the solid line in Fig. 4). The right bottom corner is assigned to high vapour pressure ILs (so-called poor ILs), where ion pairing occurs and less energy is required to remove an ion pair to the gas phase. The left upper corner is assigned to superionic ILs, where the fractional Walden rule ($\Lambda\eta^\gamma = \text{const}$) is applicable. The presence of the constant γ reflects the imbalance of energy barriers of two closely related properties, namely, viscosity and conductivity. The suitability of the fractional Walden rule means that the activation energy of conductivity is lower than the activation energy of the viscous flow. It is interesting that for the system that cannot be described by the Arrhenius law, γ represents the ratio of B parameters in the VFT equation for two processes (conductivity and viscous flow).

The crucial role of glass transition dynamics for the charge transport properties of ILs at any temperature can be demonstrated *via* scaling. Thus, the $\sigma_{DC}(T)$ curves for

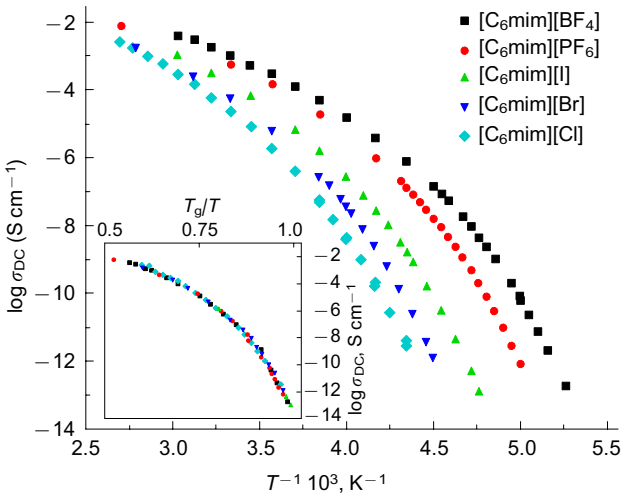


Figure 5. Temperature dependence of the DC conductivity for different ILs. In the inset, the $\sigma_{DC}(T)$ curves are scaled with respect to T_g measured by DSC. The Figure was prepared by the authors using the data from the study.[83]

different ILs plotted *vs* T_g/T do coincide (the inset in Fig. 5).[83]

It is important to mention that the absolute values of conductivity for different anions vary over 6 orders of magnitude. Moreover, the viscosity and the characteristic charge transport rate also exhibit a similar thermal activation.

One of the fundamental parameters describing the glass transition processes is the number of dynamically correlated molecules involved in transition, denoted as $N_\alpha^D(T_g)$. In 1982, Donth formulated the theoretical approach based on the fluctuation–dissipation theorem that helps one to estimate the typical size of dynamic heterogeneity *via* the $N_\alpha^D(T_g)$ quantity:[84,85]

$$N_\alpha^D(T_g) \approx \frac{N_A(1/C_p^{glass} - 1/C_p^{liquid})}{M(\delta T)^2} k_B T_g^2 \quad (5)$$

where N_A is the Avogadro constant, k_B is the Boltzmann constant, M is molar mass, C_p^{glass} and C_p^{liquid} are the isobaric heat capacities of glass and liquid at T_g, respectively, and δT is the average temperature fluctuation, which is related to the dynamic glass transition. Experimentally, δT can be evaluated by measuring the width of glass transition in the $C_p(T)$ dependence: $\delta T = \Delta T/2.5$ (ΔT is the temperature interval within which the heat capacity C_p changes from 16 to 84% of the total heat capacity step ΔC_p at T_g).

3. Glass transition temperature of ionic liquids

The glass transition temperature (T_g) is a key parameter that promotes understanding of thermodynamic and dynamic properties of liquids.[86] There are several methods to define and measure T_g, the most conventional method being DSC. It is an extremely powerful and elegant experimental tool that provides information not only on phase transitions, but also on viscosity, structural relaxation and heterogeneity. The complete description of DSC from basics to advances is available in the recent review by Zheng *et al.*[87] A step-like feature in the specific heat behaviour is observed at the glass transition temperature T_g (among many other properties). The jump in the specific heat is usually about 30–200 J mol^{-1} K^{-1}.[88] The onset of the glass transition during heating at a moderate rate of 5–20 K min^{-1} is defined as the standard T_g (Fig. 6). This means that T_g can be found as an intersection of two lines representing the linear extrapolation of $C_p(T)$ below the glass transition and the linear extrapolation of $C_p(T)$ in the region of its rapid rise during the glass transition.[87]

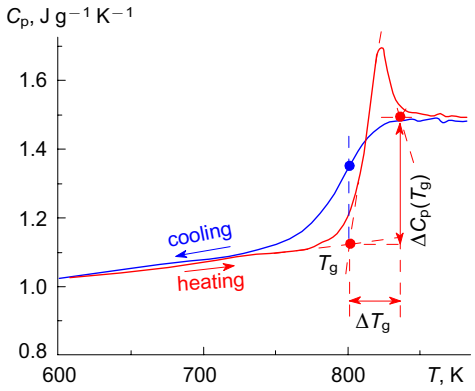


Figure 6. Temperature dependence of the isobaric heat capacity determined by DSC. The Figure was prepared by the authors using the data from the study.[87]

Different practical definitions of T_g are used, and several of them are approved as the standard ones. From the formal calorimetric point of view, the glass transition is 'the change in heat capacity, which occurs as the state of equilibrium is reestablished during warming after an initial cooling into the glassy state at a rate sufficiently high, so that no crystals have formed'.[89] In rheology, T_g is determined as the temperature at which the viscosity of the bulk sample equals 10^{13} Poise.[66] It is worth noting that such definition assumes an equilibrium state of matter and does not depend on the heating rate. In practice, the glass transition temperature of non-polymeric materials determined from the viscosity usually agrees with DSC data at heating rates from 5 to 20 K min^{-1}. The glass transition is naturally a kinetic effect. Thus, in general, the heating rate can significantly influence the resulting state of the compound. For example, at a relatively low cooling rate (1 K min^{-1}), [C$_2$mim][NTf$_2$] is transformed into a crystalline phase with [NTf$_2$] anions in cisoid conformation, while at a fast cooling rate (20 K min^{-1}), IL is converted into a glassy state with the predominance of the transoid conformers of [NTf$_2$].[90] The dependence of [NTf$_2$] conformation on the cooling rate demonstrates how the thermal history impacts the IL phase behaviour. In dielectric spectroscopy, T_g is defined as the temperature at which the structural relaxation time reaches 100 seconds. Based on dilatometric measurements and the V–T diagram, T_g is defined as the intersection point of glassy and supercooled states. Usually, all these different definitions yield different T_g values ranging within a few Kelvins.[91]

3.1. Influence of cation(anion) structure on T_g

For sure, T_g is greatly influenced by the IL structure, and a huge variety of suitable combinations of cations and anions can help in customizing ILs for specific applications. In this section, we briefly describe the main trends and strategies that can be used to control the T_g of IL *via* its structure. Variation of alkyl chain length is one of the most popular ways to gradually and predictably modify IL properties due to its synthetic simplicity and controllability.[30,92] Several studies describe the relationships between the alkyl chain length and the density, decomposition temperature, self-diffusion coefficient, conductivity, fragility and viscosity of ILs.[16,93–97] A classical T_g dependence on the alkyl chain length can be factorized into three regions in the case of [C$_n$mim][BF$_4$] (Fig. 7).[98]

The crystalline behaviour is typical of relatively short chains ($n < 3$), with relatively high melting points and less pronounced heterogeneity. The formation of good glasses and distinct heterogeneities are typical of intermediate alkyl chain lengths ($3 < n < 10$). Mesomorphism, which is influenced by an elaborate interaction balance between hydrophilic and hydrophobic parts of ILs with $n > 10$, leads to a complex crystallization behaviour and microphase separation.[98–100] Notably, imidazolium-based ILs with [Cl]$^-$ and [BF$_4$]$^-$ anions having branched alkyl chains demonstrate T_g values 15 K higher than those for linear alkyl chains and about 10 K higher than those for aromatic side groups.[96] Imidazolium- and pyridinium-based ILs with a [NTf$_2$]$^-$ anion containing ethylalkyl chains do not demonstrate a glassy state, while those with propyl chains form good

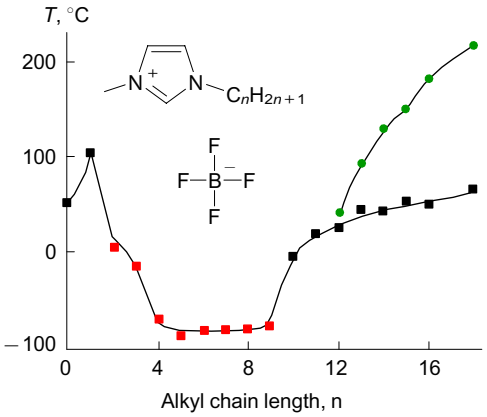


Figure 7. The dependence of phase transition temperature for $[C_n mim][BF_4]$ ILs with different alkyl chain lengths n. Red squares correspond to T_g; black squares, to T_m; green circles, to the clearing point. The solid line guides the eye. The Figure was prepared by the authors using the data from the study.[98]

glasses.[1, 101] However, ILs with $[CF_3SO_3]^-$ cannot be vitrified either upon variation of the alkyl chain length or by choosing an imidazolium or pyridinium cation.[102, 103]

The fragility is very sensitive to the anion structure, in contrast to the alkyl chain length.[94] In the case of $[C_n mim][BF_4]$, the fragility does not change significantly for $3 < n < 10$ and equals 70, which is an average value compared to other glass-formers. However, the fragility of $[C_6 mim][Br]$ is significantly higher compared to that of ILs with fluorinated anions such as $[NTf_2]^-$ and tris(pentafluoroethyl)trifluorophosphate. It was suggested that the bromide ion forms strong hydrogen bonds with the H atoms of the imidazolium cation, in contrast to the fluorinated anions, the negative charge of which is distributed over a considerable volume. Therefore, the additional hydrogen-bond network suppresses ion movement, decreases the conductivity and increases the fragility. It is also well known that aromatic moieties of imidazolium cations, especially benzyl groups, significantly change thermodynamic properties and phase transition points of ILs: T_g is greatly increased due to additional $\pi-\pi$ interactions.[104]

3.2. Glass transition temperature of IL under external pressure

An interesting interplay between the Coulomb interaction and the alkyl-chain packing can be revealed *via* the effect of external constraints such as pressure.[105] The significant role of the alkyl chain in glass formation under high pressure (up to 7 GPa) was studied in terms of conformational stability of $[C_n mim][BF_4]$.[106–108] The dominant population of the *gauche* conformers of the cation compared to the *trans* conformers suppresses the crystallization of ILs with $n > 5$ and stabilizes the system in a glassy state through alkyl chain packing. In the case of ILs with $n < 5$, the nanostructure formation is considered to be weak, and conformational stability is mainly due to Coulomb interaction. The *gauche* conformation of the cation causes a compression of the excluded volume and leads to a specific tail curling towards the imidazolium ring.[109] Remarkably, this effect is greatly influenced by the anion structure. The position of the $[BF_4]^-$ anion favours the twisting of alkyl chains and resulting changes in the liquid morphology. This is opposite to the $[NTf_2]^-$ anion that has a completely different stable location and tends to demonstrate sandwich-like structures with adjacent imidazolium cations, thus preventing alkyl chain interactions.[110] As a result, $[C_n mim][NTf_2]$ with $n = 3-10$ forms good glasses under applied pressure.[111] Fascinating, the glass transition pressure of $[C_n mim][NTf_2]$ (the pressure point at which the substance turns to a glass state at room temperature) slightly increases up to $n = 5$, remains unchanged up to $n = 8$, and rises again at $n = 10$. This is distinct from $[C_n mim][BF_4]$, the glass transition pressure of which gradually decreases, while T_g increases with increasing n.[107] Such behaviour is common to conventional glass-formers.[112,113] Moreover, $[C_n mim][BF_4]$ demonstrates additional multiple phase transitions at 7 GPa.[107] These results correlate with the fact that ILs with the $[NTf_2]^-$ anion in a liquid state have rich conformational evolution and can adapt to external perturbation.[114,115] Corresponding ILs cooperatively adjust their geometry under high external pressure, which causes substantial resistance to shear stress strength. These trends were observed for different types of cations: pyrrolidinium-,[116,117] ammonium-[118,119] and imidazolium-based ones.[111] The key feature of the $[NTf_2]^-$ anion is the charge spreading along the $O_2S-N-SO_2$ core that reduces ion-ion interactions. This results in a low energy barrier between cisoid and transoid conformers. The transoid form is slightly more stable than the cisoid one (by ~ 2 kJ mol^{-1}) (see Refs 120 and 121). Therefore, two forms typically coexist in liquid,[121–123] supercooled and glassy[121,123] states. Imidazolium-based ILs with the quite symmetric $[PF_6]^-$ anion also display complex phase behaviour under external pressure with elaborate T–P diagrams[124] and several crystalline phases (arising from $[C_n mim]^+$ conformers) supported by Raman spectroscopy.[125,126] For $[C_4 mim][PF_6]$, in addition to rich polymorphism, the unusual conformational glassy state induced by high pressure (up to 8 GPa) has been described.[127]

It is worth noting that the $T_g(P)$ dependence is strongly nonlinear both for ILs and conventional glass-formers.[128] For example, T_g of the pharmaceutically important protic IL verapamil hydrochloride increases by ~ 50 K under 350 MPa pressure, and the rate of T_g changing with pressure (dT_g/dP) equals 208 K GPa^{-1} (at ambient pressure),[129] which is comparable with that of van der Waals glass-formers but is considerably higher compared to polymeric liquids such as poly(propylene glycol) (37 K GPa^{-1}).[130]

Kinetic effects also influence the phase transitions at high pressures. The conformational changes of the $[C_2 mim]^+$ cation cause a glass transition in $[C_2 mim][CF_3SO_3]$ above 3.3 GPa at a relatively high compression rate of 1.2 GPa h^{-1}. In addition, the decompression induces crystallization at ~ 0.4 GPa, whereas at low compression rates (0.3 GPa h^{-1}) the crystal polymorphism is observed.[131] The phase of $[C_4 mim][CF_3SO_3]$ depends on the way how pressure is increased. Thus, a stepwise change to 1 GPa results in a crystalline phase, but the glassy state is reached if the final pressure point is higher, and the reliable hysteresis occurs while pressure is being released.[132]

Unusual phenomena may take place upon the release of external pressure. Some ILs, being transformed into a glassy state at high pressure, experience crystallization when the pressure is released, for example $[C_2 mim][BF_4]$, $[C_8 mim][BF_4]$ (Ref. 107) and $[DEME][BF_4]$.[133] In fact, similar behaviour has been reported for methanol, but it was found to be less reproducible.[134]

3.3. Correlation of T_g with IL molar volume

An interesting correlation between T_g and the molar volume (V_m) of IL ions can be elucidated using a cohesive energy approach.[82, 135] For an ion-counterion system disposed in the liquid, the cohesive energy represents the potential energy minimum. However, this only works for unassociated salts that obey the Walden rule. The characteristics of the potential minimum are affected by the trade-off between attractive and repulsive forces in an ion pair. The attractive forces have a complex nature of cohesive Coulomb and van der Waals interactions, which have opposite dependence on the distance: the Coulomb interaction decreases, while the van der Waals one increases with increasing ionic size. The repulsive forces are considered to arise from electron shells overlapping in the external parts of the oppositely charged ions. Therefore, the structural details of particular IL characterize the position of the cohesive energy minimum that is reflected in corresponding T_g. It is noteworthy that the sums of the effective radii can be approximated by the cubic roots of V_m. Thus, the direct connection between T_g and cohesive energy minimum can be expressed *via* the T_g *vs* V_m relation. Figure 8 shows the $T_g(V_m)$ dependence at ambient temperature for ILs with weakly and highly polarizable cations and anions.

For weakly polarizable (dashed line) ILs, a broad minimum of the T_g (and cohesive energy) is found at $V_m = 250$ cm^3 mol^{-1}, which corresponds to an inter-ionic separation of $\sim$0.6 nm.[82] This assumes a cubic packing of anions around the cations, *i.e.*, the simplest possible packing exhibited, for example, in conventional NaCl salt. It is important to emphasize the conceptual and fundamental character of the observed trends. Therefore, more details and limitations should be considered. For example, salts with aromatic cations have sufficient polarizability arising from π-electron clouds. Also, such anions as bis(oxalato)-orthoborate (depicted as [BOB] in Fig. 8), thiocyanate and dicyanamide should be considered with care, because they are highly polarizable. Interestingly, ILs based on various chelated orthoborate anions demonstrate a very stable glassy state, they do not crystallize at ambient conditions and possess significantly higher T_g values compared to corresponding salts with fluorinated anions.[135] Thus, van der Waals interactions dominate over electrostatic ones, as has also been shown for bulky large quaternary ammonium cations.[136] Figure 8 shows examples of ILs containing bis(oxalato)orthoborate with various cations; they go out of trend for weakly polarizable ILs (dashed line). Moreover, such ILs combine high T_g with high fragility and hydrophobicity. This combination of physical properties is very uncommon even for such extraordinary compounds as ILs.

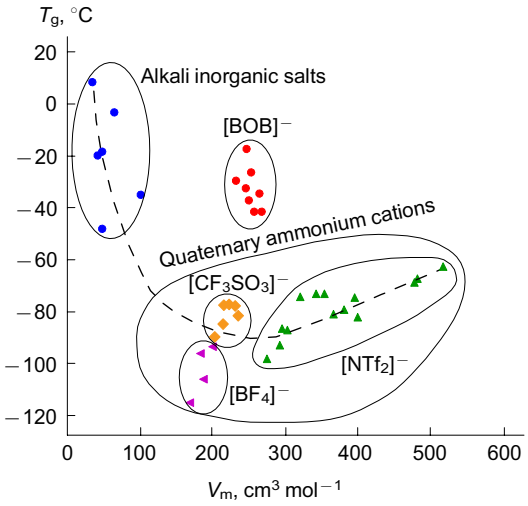


Figure 8. Dependence of T_g on the molar volume of ILs containing weakly and highly polarizable cations and anions. The dashed line through the points is a guide to the eye. The Figure was prepared by the authors using the data from the studies.[82–135]

3.4. Glass transition temperature of nanoconfined ILs

The glass transition temperature T_g is noticeably influenced by encapsulation of ILs in nanoconfinement.[137] Such materials can find broad applications as novel sensitive and stable electrodes for solid-state dye-sensitized solar cells, where proper T_g value is required for correct operation at ambient temperature.[138–141] Since the entropy decreases in confinement, a confinement-induced increase in T_g would be expected for the thermally-induced occupation of fluid-like configurational states. However, available experimental data are controversial in this regard.[137] For example, if [C$_2$mim][EtSO$_4$] is confined in the TiO$_2$ matrix, the T_g increases by 8 K.[142] In the case of imidazolium-based ILs [C$_2$mim][TsO] (Ref. 143) and [C$_2$mim][PF$_6$] (Ref. 144) incorporated in nanotubes, no difference in T_g was detected, while T_g of [C$_8$mim][Cl] decreased by 8 K in comparison with neat IL.[145] In the case of [C$_4$mim][OcSO$_4$] incorporated in a silica gel matrix, the significant reduction of the melting point T_m (52 K) with nearly zero downshift of T_g (2 K) was reported.[146] In the case of [C$_2$mim]$^+$ with [N(CN)$_2$]$^-$, [EtSO$_4$]$^-$ and [SCN]$^-$ anions confined in a mesoporous silica monolith, the T_g does not change at all, while T_m decreases by 14 K compared to the bulk.[147] Conflicting results are probably due to nominal detraction of the glass transition phenomenon in confined space, because it is a collective process, and the number of molecules involved in the transition, as well as their interaction with surroundings, should be taken into account. However, there is only one study where the accurate molecular dynamics (MD) simulation for confined IL was performed.[148] This study considered a model case, where [C$_8$mim]$^+$ tricyanomethanide was placed between two planar silica surfaces separated by a variable distance, and predicted the reduction of T_g due to such type of confinement. Interesting results on the glass transition process were obtained using spin-probe electron paramagnetic resonance (EPR) of ILs confined in the ZIF-8 metal-organic framework.[149] Significant increase in T_g (by $\sim$20 K) for [C$_4$mim][PF$_6$] and [C$_4$mim][Br] was indirectly detected; in addition, the motion of spin probes reflected the sluggish character of detected 'glass transition', which indirectly violates the classical pattern.

It is worth mentioning that the glass transition occurs in a specific way also for confined conventional solvents.[150] For example, such solvents as benzene and cyclohexane, which do not have a glassy state in the bulk, exhibit a glass transition upon confinement in mesoporous material.[151, 152] In addition, classical glass-former toluene demonstrates complex non-monotonic behaviour of its T_g in confinement depending on the silicate pore size. Thus, T_g for small pores (2.4 nm) is by 30% higher, while for intermediate pores (5 nm) it is 5% lower in comparison with the bulk glass.[153]

3.5. Glass transition temperature for IL mixtures

Yoshimura *et al.*[154] analyzed glass formation in $[C_4mim][BF_4]$ water solutions. The effect of rapid structural changes at specific water concentrations (20 and 80 mol.% H_2O) was found *via* the T_g (mol.% H_2O) plot. It was assigned to the formation of hydrogen-bonded complexes. However, at water concentrations higher than 20 mol.%, T_g behaves non-monotonically due to crystal formation. The characteristic peak at 3100 cm^{-1}, which is detected in the Raman spectra starting from 40 mol.% H_2O, is a fingerprint of water ice. Thus, a certain glass state of the mixture is debatable at such high concentrations of water. Similar phenomena were studied using MD simulation[107] and indirectly supported by the $[C_4mim][BF_4]-H_2O$ phase diagram,[155] in which critical solution behaviour at 80 mol.% H_2O was observed. The maximum water concentration for glass formation is ~90 mol.% H_2O. Importantly, the observed glass transition for $[C_4mim][BF_4]-H_2O$ mixtures was single, in contrast to the water mixtures of $[DEME][BF_4]$ showing a double glass transition[156] and well-defined T_g up to ~96 mol.% H_2O. A similar double glass transition phenomenon is also known for the classical glycerol–water solution.[157] However, the difference between two glass transition temperatures in $[DEME][BF_4]-H_2O$ is only 15 K, which is significantly smaller compared to the glycerol–water mixture (90 K). Notably, dry $[DEME][BF_4]$ displays a single glass transition temperature.[158]

The plots of T_g *vs* mole fraction of binary mixtures of many imidazolium-, pyrrolidinium- and pyrazolium-based ILs were shown to be a nearly linear.[159] The largest deviation from linearity was found for binary mixtures containing $[NTf_2]^-$ and $[Me_2PO_4]^-$ anions simultaneously; but even for them no discontinuity in T_g was observed. The combination of two ILs with the $[B(CN)_4]^-$ anion and different imidazolium and pyrrolidinium cations has a well-defined glassy state, even though one of the mixture components has no T_g in the neat state; however, such fraction should not exceed 90%.[160]

Therefore, the T_g of IL is greatly influenced by the anion and cation structure and can be qualitatively rationalized with a cohesive energy approach. The behaviour of IL glass under external pressure demonstrates abundant phenomena with mutual phase transitions and reflects the flexibility of the cation(anion) structure. The trends observed for nanoconfined IL glasses remain controversial, similar to the common glass-formers.

4. Heterogeneous structure of ionic liquid glasses

Structural heterogeneity, which manifests itself at certain conditions, is an inherent and common property of the glassy state.[35, 39, 86, 161] Supercooled liquids become dynamically heterogeneous in the vicinity of T_g, and the relaxation response results in dynamically distinguishable sub-ensembles.[34] An instantaneous snapshot consists of domains with different molecular mobility.[162] Most of the specific glass properties, such as ductility, shear modulus and relaxation response, are mutually inherited from the heterogeneous supercooled liquid state.

Heterogeneous properties of ILs play a crucial role in both the liquid and solid states of these substances.[8, 39, 163–165] Structural and dynamical heterogeneities of ILs provide their versatile properties and make ILs reasonable competitors in modern industry and academia, including such applications as green solvents, electrolytes, pharmaceuticals and functional materials. Heterogeneities can effectively modify the reaction pathways and yields, thus acting like a classical cage effect. Below we briefly describe how glass properties of ILs, which stem from their heterogeneity, are studied by different experimental approaches. We would like to mention that cryo-electron microscopy, widely used for investigation of heterogeneous structures, is not covered in this section, since its applications to glassy ILs have not yet been extensively demonstrated. At the same time, electron microscopy was already successfully applied for liquid-state heterogeneous IL water mixtures,[166] IL microemulsions[167] and IL copolymer membranes.[168] We anticipate that cryo-electron microscopy will be used to its full potential in the future to study glassy states of ILs and other IL-based materials.

4.1. Neutron and X-ray scattering

Triolo's group performed a series of insightful studies (some of them have already become classical) concerned with the dynamics of glassy and crystalline IL structures.[38,169-171] A set of fruitfully complementing calorimetry and diffraction/scattering methods have been applied to investigate the dynamics and structure of the heterogeneous glassy state in $[C_4mim][PF_6]$.[171] The relaxation dynamics of glassy $[C_4mim][PF_6]$ was probed by quasi-elastic neutron scattering (QENS). The relaxation processes at temperatures far below T_g were observed using elastic and inelastic fixed energy experiments. Three distinct temperature ranges were considered for QENS data to describe structural dynamics in $[C_4mim][PF_6]$ glass (Fig. 9).[171]

No significant structural changes occur in the temperature range of 10–100 K, where only highly localized methyl group rotation takes place (this was firstly reported by Triolo *et al.*[170]). At these temperatures, IL glass has a steady rigid structure. At higher temperatures, a very extensive and multifarious glassy dynamics takes place between 100 K and T_g (190.6 K for particular $[C_4mim][PF_6]$ (Ref. 172)), even though the diffusive motions are extremely suppressed. Methyl groups exhibit effective rotation, and the butyl chain of the cation has enough energy to yield motion between various conformations, which was investigated in detail using MD calculations.[93]

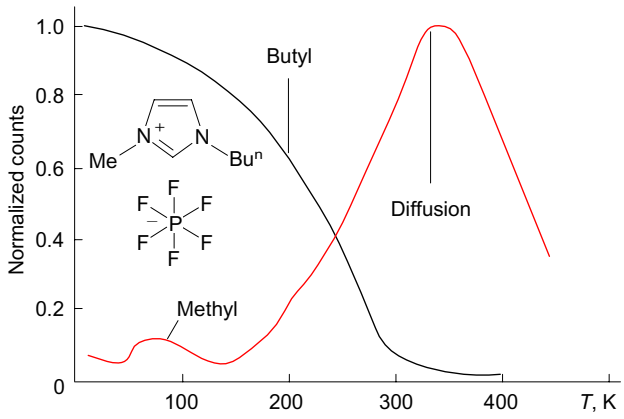


Figure 9. The data from elastic (black line) and inelastic (red line) fixed energy scattering experiments for $[C_4mim]PF_6$ in a glassy state. The characteristic temperatures for activation of the specific type of motions are depicted. The Figure was prepared by the authors using the data from the study.[171]

Notably, the relaxation for both methyl and butyl groups follows the Debye and Arrhenius temperature dependence (with single undistributed activation energies of 1.28 and 11.34 kJ mol^{-1} for methyl and butyl, respectively).[170] At temperatures above T_g, diffusive motion dominates and fully determines structural relaxation processes. Curiously, spatial correlation patterns inherited by the glass from liquid IL are clearly seen in wide-angle neutron scattering and wide-angle X-ray scattering (WAXS) experiments.[171] In particular, two intense broad peaks at 4.1 and 6.4 Å distances occur, and, similar to QENS, three distinct temperature regions for observed peak positions could be distinguished. The correspondence of these regions to those found by QENS reveals the strong connection between the activation of localized dynamics and overall morphology features in the IL glassy state.

Remarkably similar sub-T_g dynamics was observed in glassy polypropylene oxide (T_g = 210 K). Thus, the methyl group flipping begins at 150 K and gradually accompanies the entire chain motion rising above T_g.[40] However, the activation barrier for methyl group rotation in [C$_4$mim][PF$_6$] is sufficiently lower than in polypropylene oxide (1.28 kJ mol^{-1} (see Ref. 170) *vs* 14 kJ mol^{-1} (see Ref. 40). The nature of abnormally low activation energy for methyl group rotation in glassy [C$_4$mim][PF$_6$] can be revealed from its liquid state and crystal structures, in which weak hydrogen bonding is supposed according to molecular dynamics simulations.[173,174] We would like to mention that, apart from abundant physics of [C$_4$mim][PF$_6$] glass, the crystalline state can also be achieved for this IL[172] (at low cooling rates of ~0.02 K s^{-1}) with plentiful polymorphism effects that were also studied.[171]

The first experimental evidence was obtained and the quantitative description of nanostructure in glassy imidazolium-based ILs was performed using WAXS.[38] The linear dependence of the spatial correlation function peak position on the alkyl chain length reveals the existence of nanoscale ordering governed by alkyl chain aggregation: the spatial correlation rises by 2.1 Å per each CH$_2$ moiety. The temperature dependence of WAXS data for [C$_8$mim][BF$_4$] (T_g = 190 K) provides additional details about structural heterogeneity in the liquid and glassy states of the solvent (Fig. 10).

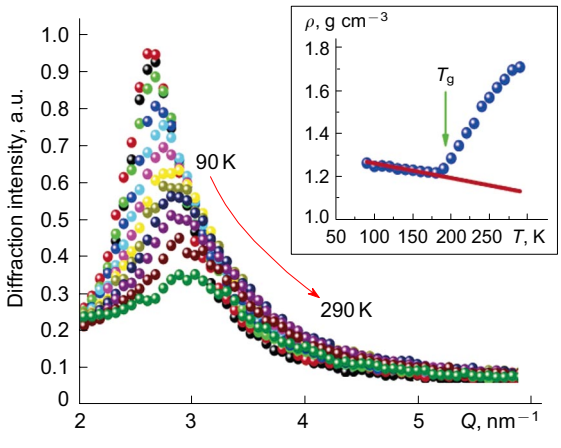


Figure 10. X-Ray diffraction patterns of [C$_8$mim][BF$_4$] at different temperatures. The inset shows the temperature dependence of the value proportional to Q^3_{max}, the red line is the extrapolation of the temperature dependence of the density. The Figure was prepared by the authors using the data from the study.[38]

The spatial correlation size ($L = 2\pi/Q$) increases with decreasing temperature below T_g. The extrapolation of the well-known density data measured for liquid [C$_8$mim][BF$_4$] yields excellent correlation with the WAXS peak position shift in the sub-T_g range, where the diffusion processes are inhibited (inset in Fig. 10). Above T_g, the interference peak shifts to higher Q with increasing temperature. In the original study,[119] this was attributed to the spatial correlation growth with decreasing temperature that is related to diffusion. Therefore, the structure and size of nanodomains in glassy IL are strongly correlated with the diffusion processes in liquid IL. The existence of a clear intermediate range order and the observed linear correlation with the alkyl chain length implies that the nanodomains are formed due to the aggregation of neutral alkyl tails.

4.2. Dielectric spectroscopy

Glassy IL dynamics and relaxation properties are being mainly investigated by dielectric spectroscopy (DS). Indeed, only DS can follow the whole evolution (18 orders of magnitude) of the system dynamics that slows down from picoseconds in supercooled and liquid states to hours and days in the glassy state. The existence and nature of secondary relaxation processes in ILs were first shown by Rossler and Rivera.[175] They studied the VFT temperature dependence of the conductivity in a series of imidazolium-based ILs with different anions and observed similarities to molecular glasses, with the ionic conductivity being the main process. Additional experiments with depolarized light scattering probed the reorientational motion of the [C$_4$mim]$^+$ cation and showed that these phenomena are interdependent and associated with the structural relaxation, which is typical of simple molecular glass-formers.[42] The impedance experiments on glassy [C$_4$mim][PF$_6$] showed the deviation of relaxation behaviour of the macroscopic electric field from viscosity and solvation dynamics, which is common for glass-formers with high fragility.[176] Optical Kerr effect spectroscopy also confirmed that the orientational dynamics of supercooled imidazolium-based ILs is similar to that of fragile van der Waals glass-forming liquids.[177,178] Solvation dynamics occurs on the time scale of structural and thermal relaxation, which was proved by reverse dynamic calorimetry.[179] However, detailed study of the ion diffusion and structural relaxations in imidazolium-based ILs revealed that the diffusion decoupling from the structural relaxation is minor in comparison with other glass-forming liquids with similar fragility. Therefore, the glass fragility is not the primary factor in defining the degree to which translational dynamics is decoupled from structural relaxation in glass-forming liquids.[180] The analysis of the acoustic phonon modes in the glassy state of [C$_n$mim][NTf$_2$] with various alkyl chain lengths showed depolarized components of Brillouin peaks for $n > 4$.[97] This is opposite to the results for ILs with [BF$_4$]$^-$ and [PF$_6$]$^-$ anions. Moreover, the activation energy for the alkyl chain relaxation process steeply increases in the dielectric loss spectra of glass ILs with [NTf$_2$]$^-$ and [BF$_4$]$^-$, which can be due to the formation of alkyl chain domains. It is worth noting that DS is useful in analyzing the IL ions in general, but it cannot give information about the dynamics of different functional groups.

4.3. Solid-state NMR

Nontrivial results on IL glass properties were obtained by NMR. There is a number of studies on IL dynamics in the equilibrium liquid state performed using NMR.[181–184] The investigation of the glassy state by NMR at cryogenic temperatures requires high-resolution solid-state NMR with high-power decoupling and magic angle spinning, which allows suppression of dipole-dipole and chemical shift anisotropy otherwise leading to a broadening and loss of information. Ionic dynamics of $[C_4mim][NTf_2]$ in liquid and glassy states has been widely studied.[171,183,185] The nano- and picosecond rotational motions were analyzed using the following four different models for the temperature dependence of the ^{13}C spin-lattice relaxation time: Bloembergen–Purcell–Pound, model-free, Davidson–Cole and Cole–Cole expressions. The most frequently used Bloembergen–Purcell–Pound model[186] implies uncorrelated isotropic random dynamics and does not fit the whole temperature range for ILs, which was also shown in other studies.[183,185] In the model-free approach, the order parameter is included due to which more information about IL molecular motion can be obtained. So, three types of motions are assumed: rotation of IL ions as a whole, slow and fast motions of local fragments. Namely, δ-CH_3 and CF_3 fragments display the fastest motion, and the mobility of the imidazolium ring is hindered in contrast to the flexible alkyl chain yielding nanosecond motion in the vicinity of T_g. Using the extended model-free approach, the temperature dependence of T_1 was described in the whole temperature range. The Davidson–Cole approach implies a spectrum of activation energies (and correlation times), so the mobile fragments possess a wider distribution in agreement with the free-model results. Several types of δ-CH_3 dynamics mean that not only axial rotation (depicted *via* the free-model approach) is responsible for ^{13}C T_1 relaxation time. The Cole–Cole model appears not applicable for this particular IL. The application of the second momentum (M_2) provides even more details on molecular mobility in the glassy state. Particularly, δ-CH_3, CF_3 and methyl groups of the imidazolium ring yield rapid axial motion with overall reorientational motion of the ring. It is noteworthy that the obtained M_2 values in the glassy state are lower than theoretical predictions, which can be rationalized by the additional motion of C–C, C–H and C–F fragments.

Solid state NMR with deuteron quadrupole coupling constant analysis provides unique information about hydrogen bonding in IL glassy media, where the proton exchange rate is slow enough to distinguish the hydrogen bonding between oppositely and like-charged ion dynamics. For a series of $[NTf_2]^-$-based ILs, it was shown that the formation of cationic clusters inhibits any crystallization process in IL. and therefore the glassy state prevails.[187–189] Interestingly, the population of cationic clusters does not change below T_g but exponentially increases above this temperature; it also significantly increases with increasing length of the alkyl chain in the cation. It is shown that hydroxyl groups in like-charged pairs are more mobile than in counter-ion ones, and the librational motion is present even at ~120 K below T_g.

4.4. Temperature-modulated DSC

As mentioned above, DSC is a very powerful tool for studying IL glasses. However, in addition to routine T_g determination, the advanced DSC can also be used for the investigation of the heterogeneous structure of IL. In this approach, low amplitude harmonic temperature oscillation is used to measure C_P.[87,190] Since the heat capacity of a heterogeneous sample is very sensitive to the thermal history, temperature modulation allows one to reveal the kinetic and dynamic contributions to thermal characteristics of the system. With this approach, the scrupulous and quantitative study of glassy IL heterogeneities was performed for a special set of protic and aprotic ILs (hydrochloride salts), and the obtained results were compared with those for corresponding neutral bases (cimetidine, tramadol, carvedilol and prilocaine).[36] Notably, the selected glass-formers have pharmaceutical applications. The reaction of these drugs with HCl resulted in their transformation into the protic IL form; in fact, the drug transforms into an HCl salt. In each chloride–base pair, the molecules have almost identical chemical structures, but their intermolecular interactions are completely different. The classical Lennard-Jones intermolecular potential is applicable to bases. For their ionic counterparts, long-range intermolecular electrostatic interactions play a major role and dominate over the van der Waals and hydrogen-bonding interactions. Thermal analyses of selected compounds provided very interesting results. Thus, the number of dynamically correlated molecules involved in the glass transition process, $N_\alpha^D(T_g)$, for IL is significantly smaller compared to the bases. Therefore, the increased width of the glass transition in the $C_p(T)$ plot for IL dominates at their higher T_g values in comparison with corresponding bases (see Eq. (6)).

Figure 11 shows a clear linear correlation between the ratio of the $N_\alpha^D(T_g)$ for a base and IL and the molecular weight of its cation.[36] Here, the molecular weight is the measure of molecular complexity, so the characteristic size of heterogeneity is significantly influenced by ion topology. The prevailing role of the Coulomb interaction leads to the reduction of intermolecular distances in the vicinity of T_g. Contrary to that, the dipole-dipole interactions play a major role in neutral bases and cause a growth of heterogeneity

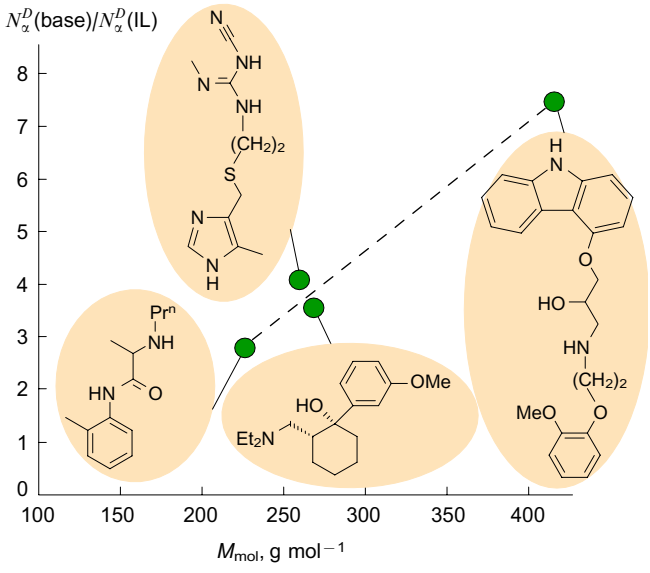


Figure 11. The correlation between the ratio of the $N_\alpha^D(T_g)$ for a base and IL and the cation molecular weight. The Figure was prepared by the authors using the data from the study.[36]

and T_g spreading. The values of $N_\alpha^D(T_g)$ vary for different kinds of glass-formers in the range of 70–200 for hydrogen-bonded liquids and 80–300 for van der Waals liquids.[191,192]

4.5. Electron paramagnetic resonance

Recently, EPR spectroscopy has been fruitfully employed to study heterogeneities in IL glasses. The necessity of using paramagnetic probe molecules makes this approach significantly different compared to the other above techniques. One can suggest that any phenomenon observed *via* EPR in IL can be triggered by a probe and specific solute–solvent interactions cannot be excluded (*e.g.*, even trace amounts of water can dramatically change physical properties of IL[193–196]). However, the majority of IL applications assume using IL not in the neat form, but rather as a medium for task-specific molecules; therefore, the probe-based technique is appropriate in revealing heterogeneous properties of ILs.

A versatile and complex EPR approach was developed to study heterogeneous structural rearrangements in glassy ILs.[43,149,197–200] It was found that pulse EPR is sensitive to stochastic small-angle wobbling of spin probes located in glassy media. The temperature dependence of the librational motion parameter $L(T)$ is a very informative characteristic of such molecular mobility. It reflects the angular amplitude of spin probe motion at a certain temperature. It is important to note that this approach was used to study a variety of objects: organic glasses[201,202] (water–glycerol mixture, dibutyl phthalate, trehalose and squalane), 1,2-dipalmitoyl-sn-glycero-3-phosphocholine[203,204] and 1-palmitoyl-2-oleoyl-sn-glycero-3-phosphocholine[205,206] model biological membranes. Moreover, the observed dynamic transition temperatures of and basic structural correlations for purple membranes were independently reproduced by Raman[207–209] and elastic incoherent neutron scattering[210,211]/QENS[212] spectroscopy, as well as by MD.[213] In our work, the above-mentioned libration-based approach was implemented for the first time to study heterogeneous dynamics of glassy ILs. A variety of imidazolium- and pyridinium-based aprotic IL glasses were studied, and, in general, the behaviour of the $L(T)$ curve can be described by factorizing it into three characteristic temperature regions (Fig. 12).

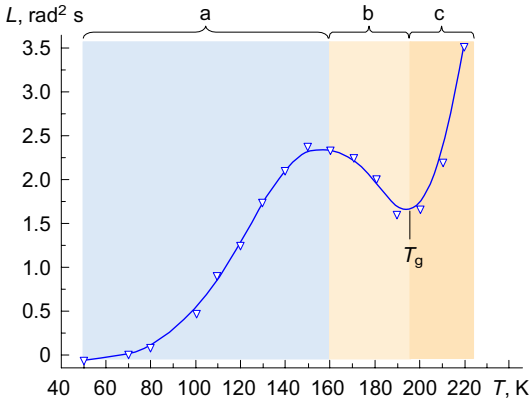


Figure 12. Temperature dependence of the librational motion parameter for nitroxide radical dissolved in IL. The line through the points is a guide to the eye. The Figure was prepared by the authors using the data from the study.[198]

The first region (a) that starts with the rise of the $L(T)$ function at ~70 K and ends at temperatures ~(T_g – 60 K), shows the classical linear growth of L *vs* T that has been previously observed for organic glasses and lipid bilayers in the above-mentioned studies. The slope of the $L(T)$ curve characterizes the local rigidity of glassy media, and the onset point reflects the activation energy required for the wobbling of the spin probe. Next temperature region (b) extending from ~(T_g – 60 K) to T_g, reveals the suppression of stochastic molecular librations with the temperature growth. The reduction of librations assumes that the glassy matrix becomes harder with temperature. This behaviour is not typical for the majority of substances, therefore, it was called a 'structural anomaly'. It was suggested that this anomaly can only arise from the effect of solvent molecules surrounding the dissolved nitroxide radical and relates to specific structural rearrangements. The last region (c), covering temperatures above T_g, reflects the transition from small-angle librational motion to the free diffusive rotation of spin probe, where the theoretical approach used cannot be applied any longer. We studied the structural anomaly in a variety of imidazolium-based IL glasses ([$C_n$mim][BF_4]) with different alkyl chain lengths.[200] Surprisingly, a clear correlation was found between the observed anomaly and the dependence of T_g on the alkyl chain length (see Fig. 7). One can assume that the detected anomaly can be induced and governed by the spin probe geometry and magnetic properties. However, it was demonstrated that the $L(T)$ curve does change for another spin probe used: trityl radical instead of nitroxide one.[214] Compared to nitroxides, trityl radicals have completely different geometry (hydrodynamic radius of ~7 Å (Ref. 215) *vs.* ~3.4 Å (Ref. 216)), relaxation properties such as the spin–spin relaxation time T_2 (~10 μs at 300 K in a water solution[217] *vs* ~0.3 μs at 210 K in a water–glycerol (1 : 1) solution[218]), the radical center (C–C moiety *vs* N–O moiety), the nature of dominating anisotropy (g-tensor *vs* hyperfine interaction) and, as a consequence, different EPR spectra. Therefore, it was proved that the observed structural anomaly reflects the inherent property of IL glass. The necessary and sufficient criteria for the occurrence of the anomaly in glassy media were formulated: the alkyl chain length should be $3 < n < 9$ (for proper glass formation) and the T_g should be not less than ~175 K (to let the alkyl chains govern structural rearrangements before glass transforms into liquid). One would mention that not only IL glasses can satisfy these conditions. Indeed, we can observe the anomaly in a glass of the traditional plasticizer dibutyl phthalate as well.[200] This fact emphasizes the generality and fundamental meaning of the discovered anomaly, which aids in the understanding of dynamics and relaxation processes in glasses. It was also demonstrated that the ideal macroglassy state is not an absolutely necessary condition. The IL–H_2O mixture with a water content of up to 50 wt.% reveals a similar anomaly despite the fact that the mixture is amorphous at the macro level.[199] Furthermore, the spatial dimensions required for cooperative anomalous rearrangements can be estimated via incorporation of IL molecules into the cavity of a metal-organic framework (*e.g.*, ZIF-8). As a result, the $L(T)$ curve is reasonably modified, and for some ILs the anomalous rearrangements can be completely inhibited, being attributed to specific molecular packing in confinement.[149]

4.6. Molecular dynamics

Nowadays, molecular dynamics is extensively used to study the heterogeneous nature of ILs in the liquid state and to support the corresponding experimental data,[8,10] whereas the studies in glassy IL states are less common. Habasaki and Ngai[219,220] performed a detailed research on heterogeneous structure of glassy $[C_2mim][NO_3]$ using an all-atom model. In particular, the ion mobility in the vicinity of T_g was found to be similar to conventional glass-forming liquids with specific suppression of ion diffusion jumps, as was revealed in the VFT-type temperature dependence of the diffusion coefficient (see Eq. (3)).[221,222] A multidomain structure at several distinct scales of length and mobility was found and quantitatively compared with the Li-ion metasilicate glass Li_2SiO_3. At the same time, the complex slowdown of the dynamics in a glassy network was observed, which was evidenced by the formation of widely distributed fictive bonds with polyhedral symmetry and by a simultaneous decrease in degrees of freedom in the vicinity of T_g.[223] There are some studies related to the analysis and successful prediction of T_g values based on viscosity and conductivity data for pure[224–226] and polymerized ILs.[227] However, in general, MD studies of IL glasses and supercooled states still remain scarce and have been applied only to a limited number of ILs. In summary, this section demonstrates that heterogeneous properties of ILs can be revealed at various time or space scales and can be studied by a number of experimental techniques, as well as theoretical approaches. The dynamics of the glassy state is mainly governed by complex dynamics of methyl groups, which is accompanied by entire cation(anion) motion and collective matrix rearrangements. Apart from the distinguishing features described above, similar trends are common to any glass-formers. Below, the main applications of ILs are highlighted, where the knowledge of glass properties is crucial and decisive to promote ILs in the corresponding areas.

5. Pharmaceutical applications

In general, the successful development and production of drugs require several interdependent conditions to be simultaneously satisfied, such as molecular mobility (solubility), chemical stability and selective activity. A significant part of pharmaceuticals used worldwide is amorphous, *e.g.*, peptides, proteins and low-molecular-weight drugs. A key obstacle to meeting the above requirements by amorphous forms is their spontaneous crystallization. At the same time, the amorphous form offers better bioavailability. In addition, the physical stability of amorphous compounds is tightly related to molecular mobility and relaxation properties in supercooled and glassy states. Therefore, the knowledge of glass transition properties is a significant milestone in revealing possibilities of pharmaceutical application of compounds.[228–230]

Three generations of ILs can be distinguished according to their key properties and applications that they are focused on. The first generation of ILs was focused on basic physicochemical properties, such as viscosity, solubility, conductivity, density and thermal stability. The second generation arose from the targeted synthesis that was requested from specific industrial applications, such as lubricants, extraction and separation in catalytic reactions, eco-friendly properties. The modern rise of the third generation is especially focused on medical and biological applications.[231–233] Ionic liquids demonstrate a thermodynamically stable phase and avoid environmental polymorphism; the combination of active pharmaceutical ingredients with ILs (API-IL) can greatly improve solubility and dissolution rates; the dual functionality using active anions and cations can be pursued. Because of that, such substances attract significant attention in scientific and industrial communities.[231,234,235] Regarding the biological activity of ILs in the context of pharmaceutical applications, there are several comprehensive reviews that entirely cover the topic.[3,5]

Since the stability of pharmaceuticals depends on the mobility in the glassy state, the majority of related articles are focused on the relaxation behaviour.

The mixing of practically water-insoluble ibuprofen with the $[C_2OHmim]^+$ cation[236] leads to the API-IL compound with water solubility being 10^5 times higher than that of the initial ibuprofen. The T_g of $[C_2OHmim][Ibu]$ is very sensitive to the water content and gradually increases through dehydration.[237] In addition, water greatly enhances the ionic conductivity of the medium. The compound $[C_2OHmim][Ibu]$ demonstrates the complex relaxation behaviour in glassy and super-cooled states: on the one hand, extensive dipolar reorientations, common to conventional glass-formers, are detected; on the other hand, the conductivity process (typical of ILs) is strongly related to α-relaxation and dominates over other types of relaxation.

The slow molecular dynamics of three API-IL compounds such as lidocainium docusate [LID][Doc], didecyldimethylammonium ibuprofenate [DDA][Ibu] and choline ibuprofenate [CHOL][Ibu] was studied using thermally stimulated depolarization currents and DSC.[238] The API-IL compounds [DDA][Ibu] and [LID][Doc] did not crystallize upon slow cooling and transformed into the glassy/amorphous solid state upon shock-freezing, whereas [CHOL][Ibu] does form a crystalline state. The thermally stimulated depolarization current experiments show two relaxation peaks for [DDA][Ibu] and [LID][Doc]. The low-temperature peak corresponds to a glass transition and has a shape usually observed for strong glass-forming liquids, which was additionally supported by the temperature dependence of the relaxation time. The second peak at $\sim 1.3\,T_g$ reflects the glass-to-metastable liquid phase transition with the freezing of orientational polarization. This behaviour differs from that of molecular liquids, in which the freezing of polarization above T_g does not occur. Interestingly, no secondary relaxation was detected in [DDA][Ibu] and [LID][Doc] *via* thermally stimulated depolarization currents, indicating that local motions in glassy API-IL involve nearly apolar molecular groups that are silent in dielectric techniques.

Analyses of glassy states for two protic API-IL, procaine hydrochloride and carvedilol phosphate revealed the decoupling of ion diffusion and molecular rotational motion below T_g.[239,240] It was also approved that the aging rate is defined by the slow structural relaxation dynamics of the glass, a common behaviour that was studied for another pharmaceutical IL, lidocaine hemisuccinate.[241]

Thus, the pharmaceutical applications of ILs are active within the modern growing field of API-IL. The knowledge of IL glass transition properties helps to quantitatively determine the stability of API-IL, thus being a lighthouse directing the target synthesis of these promising compounds.

6. Cryopreservation applications

Finding suitable conditions for enhanced chemical and physical stability is an important issue for many biological objects, and one of the solutions — glassy state storage — strongly depends on the possibility of glass formation and corresponding significant reduction of molecular mobility.[242–244] Also, the investigation of basic biological systems in the glassy state gives a new understanding of the mechanisms of biological stability at extremely low temperatures.

There is a challenge in the preservation of recombinant proteins without inhibiting reagents. In this manner, the glassy state looks like a perfect preservation condition.[244] Unfortunately, aqueous solutions of common anti-aggregation agents (guanidine hydrochloride and urea) possess strong ice formation and cannot form glass. Conventional cryoprotectants such as DMSO, glycerol and sugars serve to suppress the crystallization and inhibit structural changes of proteins. However, they often stimulate aggregation processes and temperature-induced membrane damage,[245] as well as exhibit toxicity.[246]

An exciting quality of aqueous IL solutions is that they readily form a good glass over a broad range of IL concentrations, up to mol.% IL > 10, while T_g values remain in a range of 160–180 K for up to mol.% IL = 100.[154,247] Therefore, aqueous IL solutions possess cryopreservation properties and can be competitive with conventional cryoprotectants. They form an excellent glassy state and inhibit aggregation, but sometimes can induce tricky structural transitions of proteins. The direct interaction of specific amino acid moieties with the IL cation and anion is a key process in protein structural rearrangement,[248,249] and this effect is only intensified in the solvent glassy state. For example, a water solution of 1-butyl-3-methylimidazolium nitrate ([C_4mim][NO_3]) at an IL concentration of up to 6 M can induce unfolding of chicken egg white lysozyme. This occurs due to an α-helix destruction by the NO_3-anion, particularly due to the interaction with the Tyr residue. However, lysozyme stays completely non-aggregated and keeps a partially globular state at higher [C_4mim][NO_3] concentrations, above 10 M.[250] Another approach to cryopreservation and activity of chicken lysozyme at cryogenic temperatures in glassy ILs was used for [C_4mim][Cl] and ethylammonium nitrate (EAN) water mixtures that interact with Tyr, Pro, Phe and Ala, Val residues, respectively.[247,251] Despite the formation of a perfect glass and the absence of lysozyme aggregation, the water [C_4mim][Cl] mixture disrupts the protein structure. This is in contrast to EAN mixtures, in which the protein structure was retained up to high EAN concentrations, but cold crystallization effects occurred. These controversial results were interpreted in a way that interacting site residues cover the entire lysozyme molecule. Therefore, lysozyme structural stability and activity are higher after cooling than before cooling, thus allowing the protein structure to remain preserved even in a non-prefect glassy solvent.

Takekiyo *et al.*[252] compared the cryoprotective properties of DMSO and IL using bovine heart cytochrome c. Water mixtures of the protic IL EAN and aprotic 1-butyl-3-methylimidazolium thiocyanate ([C_4mim][SCN]) were studied over a wide range of IL concentrations. It is essential that while both ILs cause protein denaturation, >90% of activity and the structure were recovered after cryopreservation (X > 10 mol.% IL) followed by the removal of ILs by dialysis. The final recovery is higher compared to that using DMSO. However, the activity and structural stability of cytochrome c in aqueous IL solutions are lower than those in aqueous DMSO solutions. Authors emphasize the significant stabilization of the protein structure by the protic IL EAN in comparison with aprotic imidazolium-based ILs. The potential to study other alkylammonium-based ILs that mimic natural protein fragments was proposed and investigated in their subsequent research.[253] A series of alkylammonium-based ILs with different alkyl chain lengths (methylammonium nitrate, EAN and propylammonium nitrate) were examined aiming to understanding whether or not they possess helix-forming ability for a selected list of model proteins (ribonuclease A, β-lactoglobulin, ubiquitin, α-lactalbumin and cytochrome c) without protein aggregation. In general, the helix-forming ability correlates with the low polarity of used protic ILs. Concentrated aqueous solutions of ILs cause protein unfolding; however, EAN and propylammonium nitrate glasses induce helical formation. On the contrary, methylammonium nitrate mixtures did not trigger the formation of the unnatural helical structure of the five model proteins.

The most intriguing suggestion is that protein stability in glassy aqueous solutions of ILs correlates with the nano heterogeneous structure of the corresponding liquid solutions, *i.e.*, that the heterogeneous structure governs the stability of the dissolved protein.[250] A similar effect was investigated using bovine milk β-lactoglobulin (β-LG), in which aqueous glassy solutions of [C_4mim][NO_3] and [EAN][NO_3] induced the α-helical structure formation at high IL concentrations.[254]

It is well-known that a high cross-β-sheet content triggers the aggregation of misfolded proteins into the amyloid form. Amyloid aggregates participate in many neurodegenerative diseases, in particular Parkinson's disease. For the development of modern neuro medications, it is necessary to address the basic challenges of amyloid dissolution and refolding, as well as the preservation of recombinant proteins.

A series of different aqueous glassy mixtures of ILs were investigated as cryopreservation agents for bovine insulin amyloid with high dissolution/refolding properties and aggregation inhibition.[19] Among six tested ILs, insulin refolding ability was based on the refolded α-helical fragment, and [C_4mim][Cl] showed the best results among DMSO and the other used ILs. It was shown that the refolding ability of ILs strongly correlates with their dissolution ability.

The high level of basicity in hydrogen-bonded ILs triggers the destruction of intermolecular hydrogen bonding in insulin amyloid in the case of concentrated aqueous IL mixtures. Interestingly, in this case, imidazolium-based ILs have greater dissolution ability compared to ammonium-based ILs or DMSO. Moreover, 80% recovery after cryopreservation was achieved for the secondary structure of insulin amyloid dissolved in an IL aqueous solution. Notably, [C_4mim][Cl] demonstrated 90% recovery of the insulin secondary structure.

One of the promising applications of ILs in biology is the design of task-specific ILs based on amino acids — so-called amino acid ionic liquids (AAILs). Amino acid as a functional platform brings its unique properties such as biodegradability and biological activity in newly synthesized AAIL. Ohno and Fukumoto[255] studied twenty different natural amino acids as anions, to be coupled with the

$[C_2mim]^+$. Assuming possible cryopreservation applications of created ILs, the glass transition temperatures were investigated as well. First, all AAILs possess T_g and do not crystallize. Notably, T_g of these AAILs is mainly influenced by the side group of the carboxylic acid residue, and final T_g values vary in a wide range from −65 to 6 °C. The ionic conductivity of liquid AAIL and its T_g are inversely proportional, because the ionic conductivity (*i.e.*, ion mobility) is influenced by the viscosity of the ion conduction path, and a solvent with lower T_g has faster ion migration at an ambient temperature. But for several AAILs the opposite trend was observed, *i.e.*, the introduced functional group played a role of a hydrogen bond acceptor or donor and disturbed intramolecular interactions, resulting in the decrease in the ionic conductivity. For the majority of synthesized AAILs, the viscosity and T_g were found to be lower compared to those of the corresponding $[C_2mim]^+$-based salts. The variation of the alkyl chain length confirms one more general rule for all AAIL glasses and super-cooled liquid states: T_g consistently grows (and the viscosity as well) upon elongation of the alkyl chain of amino acid.

Thereby, cryopreservation applications of ILs are related to their glassy and supercooled states. Thus, unique heterogeneous properties and specific interaction sites make IL glasses competitive with conventionally used cryoprotectants. For sure, further investigations of the biological activity of ILs in the liquid state and physicochemical properties in the glassy state should promote IL application in this field.

7. Polymerization and energy applications

7.1. Plasticizer effect

Polymer chemistry is the field, in which ionic liquids have found a lot of applications. They can be used as polymerization media [256, 257] including atom transfer radical polymerization,[258] ionic and coordination polymerization,[259] electrochemical polymerization.[260] Imidazolium- and ammonium-based ILs are widely used as starting materials for novel polyelectrolyte synthesis. Various ways to initiate polymerization were applied, *e.g.*, thermal initiation,[261] photoinitiation [262] and UV-initiation.[263]

Generally, ILs as solvents inhibit side reactions helping to separate the polymer product from the catalyst, increase the k_p/k_t ratio, and, regarding the glass state properties, lower T_g of synthesized polymers. Therefore, ILs are used as plasticizers — additives that make polymers workable and flexible at low temperatures. Widely used poly(vinyl chloride) (PVC) can be modified by IL as a plasticizer, and impacts of a wide range of ammonium-, imidazolium- and phosphonium-based ILs were studied.[48] As a result, the PVC flexibility was greatly increased. Thus, the elastic modulus at ambient temperature decreased and the elongation at break increased by 50% or more. Meanwhile, in comparison with conventional plasticizers (mainly phthalate esters), the UV stability of PVC with IL does not significantly change, but the high-temperature stability, leaching and migration properties are considerably improved. Poly(methyl methacrylate) modified with imidazolium-based ILs demonstrates linear T_g dependence of the IL weight content, in contrast to an almost steady trend observed for dioctyl phthalate (Fig. 13).[45, 264] Pure PMMA has $T_g \approx 120$ °C, which can be decreased to 40 °C with 50 wt.% IL.

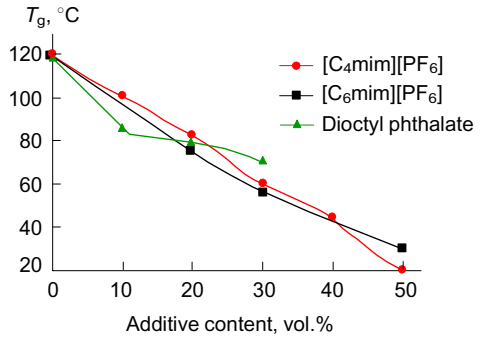


Figure 13. Data on T_g of PMMA modified with ILs and dioctyl phthalate for comparison. The line through the points is a guide to the eye. The Figure was prepared by the authors using the data from the studies.[45, 264]

The T_g of the aprotic and protic polymerized ILs are noticeably higher compared to the that for IL monomers used for their production, which is extremely important in the film formation for coating applications.[261, 265] Polymerized IL methacrylates demonstrate a pronounced effect of T_g reduction with increasing size of the alkyl substituent at the cation, and this effect is stronger in comparison with IL methacrylates.[263] For example, the variation of substituted polymer segments from methyl to hexyl leads to T_g change by 11 K for monomers and by 27 K for polymers. Furthermore, T_g values of the polymerized IL methacrylates were more than 70 K higher compared to the corresponding monomers.

The water content significantly influences the T_g and conductivity phenomena in polymerized ILs, as was demonstrated with the protic IL 1-(4-sulfobutyl)-3-vinylimidazolium trifluoromethanesulfonate $[HSO_3-BVIm][OTf]$ *via* a complex methodology employing DS and temperature-modulated DSC.[262] The glass transition temperature strongly decreases upon water addition (Fig. 14).

The sample, which was dehydrated *in vacuo* but not annealed at high temperature, still contains ∼2 wt.% of water, and total drying (with possible decomposition) is achieved only under high-temperature heating. The addition of 11 wt.% of water leads to dramatic T_g change by

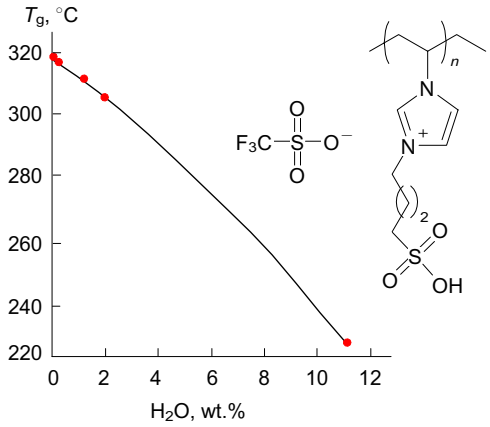


Figure 14. Dependence of T_g on the water concentration for polymerized imidazolium-based protic IL $[HSO_3-BVIm][OTf]$. The line through the points is a guide to the eye. The Figure was prepared by the authors using the data from the study.[262]

almost 100 K. Water addition largely increases the polymer conductivity; moreover, at room temperature the absolute value of conductivity in a dried sample is even lower than that in non-polymerized [HSO_3-BVIm][OTf]. At the same time, $\sigma_{DC}(T_g)$ remains unchanged with water concentration, which can be explained by the domination of the fast proton hopping mechanism of charge transport.

Regarding the place of IL glasses in polymer science, ILs as additives play a supportive role, improving the mechanical and conducting properties of commonly used polymers. However, taking into account an almost infinite number of possible cation/anion combinations, the current development of polymerized ILs and their interesting conducting conductive properties suggests great prospects for future research.

7.2. Solid-state electrolytes

There is a great demand in non-flammable and non-volatile solid-state electrolytes that can be shaped and designed for particular application requirements.[266–268] Ionic liquids are promising as electrolytes due to their inherent properties, huge structure/property variability and outstanding thermal stability; therefore, they represent a potent platform for the development of modern solid-state electrolytes.[2, 269, 270]

Gel polymer electrolytes are most extensively studied among all types of solid-state electrolytes.[269, 271] Gel polymer electrolytes based on ILs, called *ionogels*, have attracted considerable interest during the past two decades.[6, 46, 47, 270, 272–274] Regarding the glassy state properties, the T_g value is vital for electrolyte conductivity performance. Ionogel is a self-consistent binary complex of IL and net polymer. Therefore, its T_g value lies between corresponding T_g values of the used components. In general, the mixing of a conducting salt with a polymer drops down the conductivity, which also leads to an increase in T_g compared to the bulk conducting component. In this regard, the T_g of electrolyte is a marker of its conductivity at any temperature, and lowering of T_g is a general strategy for the design of novel electrolytes. Consequently, the problem of decreasing ion mobility can be solved by adding a component with low T_g. That is why ILs, which mainly possess low T_g values, high stability and conductivity and exhibit favourable plasticizer effects, are appropriate candidates for solid-state electrolytes.[23, 54, 275]

The ionic conductivity in the liquid state correlates with T_g: the conductivity increases as T_g gets lower regardless of the carrier ion type.[276] This trend is demonstrated and described in Fig. 3.

For example, the mixing of PMMA with [C_2mim][NTf_2] strongly affects T_g, which decreases as the mole fraction of IL increases (the left axis in Fig. 15); the conductivity reaches 10^{-2} S cm^{-1}, which is comparable with those of liquid electrolytes.[47] Interestingly, due to a drastic difference in the diffusion coefficients of $[C_2mim]^+$ and $[NTf_2]^-$ in such kind of ionogels, the total number of carried charges non-monotonically varies with molar fraction of IL (the right axis in Fig. 15).

A composite of MMA with [C_4mim]PF_6 demonstrates $\sigma \sim 10^{-2}$ S cm^{-1} and $T_g = 296$ K with the optimum ratio of components being 1 : 1.[277] A wide range of conducting polymerized ILs based on *N*-ethylimidazole with different polyanions was investigated, demonstrating $\sigma \sim 10^{-4}$ S cm^{-1} at room temperature with corresponding $T_g = 178$ K for optimized compound.[55] In another study it was shown that the addition of 10% mol [C_2mim][BF_4] to the Li^+-ion glass electrolyte $50Li_2SO_4{\cdot}50Li_3BO_3$ led to a decrease in T_g by 50 K and a simultaneous increase in the conductivity by up to three orders of magnitude (to 10^{-4} S cm^{-1}).[278]

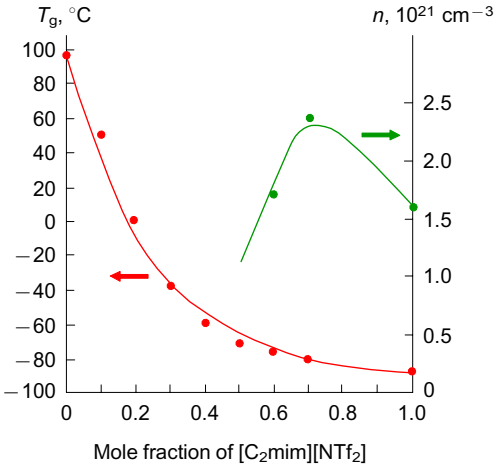


Figure 15. Dependence of T_g on the molar fraction of [C_2mim][NTf_2] in PMMA polymer-based ionogel (left axis, red symbols). The dependence of the number of ion carriers on the molar fraction of [C_2mim][NTf_2] in PMMA polymer-based ionogel (right axis, green symbols). The lines through the points are guides to the eye. The Figure was prepared by the authors using the data from the study [47].

The addition of ILs to modified poly(ethylene oxide) — one of the most popular hosts for conducting polymers — greatly increases the ionic conductivity, which is mainly controlled by carrier-ion mobility rather than by the lattice energy. A very strong plasticizing effect was demonstrated for a single Li-ion conducting polymer based on poly[(4-styrenesulfonyl)(trifluoromethyl(S-trifluoromethylsulfonylimino)sulfonyl)imide] ([PSsNTf$_2$]) and poly(ethylene oxide) with $T_g = 317$ K, the lowest glass transition temperature being observed for neat Li ionomers.[279] There are several studies, in which the lithium salt Li-NTf_2 was mixed with zwitterionic IL,[280] poly(ethylene oxide-co-propylene oxide), PMMA[281] or modified by silica nanoparticles.[282] Therefore, the ionic conductivity of ionogels is generally higher than that of ordinary polymer electrolytes. It was found that a mixture of zwitterions with the Li-NTf_2 salt demonstrates the highest ionic conductivity and simultaneously the lowest T_g, which confirms the above-mentioned trend.[51] The conductivity of ionogels for the optimal polymer : IL ratio is $\sigma \sim 10^{-4}$ S cm^{-1} at 373 K in all the cases mentioned above.

The study of stable polymer electrolytes based on the imidazolium polyanion/polycation ILs with a vinyl spacer showed a sufficient decrease in T_g after polymerization and a similar correlation between T_g and ionic conductivity.[55] An interesting study was performed in attempting to develop IL, in which ions cannot migrate along the potential gradient — a wide list of mixtures of 45 zwitterions with lithium salts was analyzed.[280] Despite the high melting points of zwitterions (> 373 K), the sample with $T_g = 236$ K and $\sigma \sim 10^{-3}$ S cm^{-1} at 373 K was obtained for the sulfonate-containing zwitterion with the Li-NTf_2 salt.

It is worth noting that DS data help to determine the mechanism of the charge transport for polymeric ionic conductors. For example, if the fast proton hopping

through a hydrogen-bond network dominates over viscosity-controlled molecular diffusion, the decoupling of ionic conductivity from the structural relaxation should occur in the vicinity of T_g. In other words, intense ionic motion coexists with suppressed structural relaxation and strongly correlates with the ionic conductivity.[283] Formally, such decoupling is revealed in the change of the temperature dependence of conductivity from VFT (Eq. (4)) to the Arrhenius model above and below T_g, respectively. The mentioned crossover was found for polymerized low-molecular-weight protic ILs.[284,285] The dielectric and viscoelastic data for imidazolium-based polymerized ILs with $[NTf_2]^-$ and $[BF_4]^-$ counterions and different side chain lengths revealed that the lowest T_g (and the highest conductivity) can be achieved with $[NTf_2]^-$ and $[BF_4]^-$, tending to a strong aggregation.[286] As the alkyl chain length increases, the ions become spaced, which lowers T_g and increases the dielectric constant.

8. Conclusion

This review summarizes a variety of data on physicochemical properties of ionic liquid glasses, *i.e.*, ionic liquids in their glassy states. In particular, the main trends of fundamental glass parameters such as T_g and fragility and their relationship with the IL structure are described. The unusual observations for the IL glass behaviour under external pressure, nanoconfinement and mixing are highlighted. The distinctive IL property, a heterogeneous structure, is even more emphasized in the glassy state. Main experimental approaches allowing the investigation of heterogeneities in IL glasses are discussed. Various scattering techniques, magnetic resonance and calorimetry reveal the diverse physics of IL glasses over a broad range of temporal and spatial scales. It is well known that ILs hold promise for a great number of applications due to their unique heterogeneous properties, which was thoroughly described in previous reviews. In the current one, we attempted to interconnect the supercooled and glassy IL properties and underline their unique stand in the context of particular applications. In particular, we demonstrated the great potential of IL glasses especially as cryoprotectants, in which specific interaction sites with proteins, mutual combination of IL with amino acids and stable glassy states opens vistas for real practical use. Moreover, the supportive role of ILs in the improvement of PVC/PMMA glasses and mechanical stability of API-ILs cannot be underestimated. Computational (*e.g.*, molecular dynamics) studies of IL glasses are scarce so far, especially in the case of complex systems with proteins and polymers. This is a challenge for future research, which would provide additional information and strongly aid in improving the existing knowledge in this field.

The review was written with the financial support of the Russian Foundation for Basic Research (Project No. 20-13-50340).

9. List of acronyms and designations

AAIL — amino acid ionic liquid;
API-IL — active pharmaceutical ingredient – ionic liquids;
BOB — bis(oxalate)orthoborate;
DEME — *N*,*N*-diethyl-*N*-methyl-*N*-(2-methoxyethyl) ammonium;
DS — dielectric spectroscopy;
DSC — differential scanning calorimetry;
EAN — ethylammonium nitrate;
EPR — electron paramagnetic resonance;
$[HSO_3-BVIm]$ — 1-(4-sulfobutyl)-3-vinylimidazolium;
Ibu — ibuprofenate;
IL — ionic liquid;
m — fragility index;
MD — molecular dynamics;
mim — methylimidazolium;
NTf_2 — bis(trifluoromethane sulfonyl)imide;
OTf — triflate;
PMMA — poly(methyl methacrylate);
PVC — poly(vinyl chloride);
Py — pyridine;
QENS — quasi-elastic neutron scattering;
T_g — glass transition temperature;
T_m — melting point;
TsO — tosylate;
VFT — Vogel – Fulcher – Tammann equation;
WAXS — wide-angle X-ray scattering.

10. References

1. N.V.Plechkova, K.R.Seddon. *Chem. Soc. Rev.*, **37**, 123 (2008)
2. M.Watanabe, M.L.Thomas, S.Zhang, K.Ueno, T.Yasuda, K.Dokko. *Chem. Rev.*, **117**, 7190 (2017)
3. I.M.Marrucho, L.C.Branco, L.P.N.Rebelo. *Annu. Rev. Chem. Biomol. Eng.*, **5**, 527 (2014)
4. T.Welton. *Chem. Rev.*, **99**, 2071 (1999)
5. K.S.Egorova, E.G.G.Gordeev, V.P.Ananikov. *Chem. Rev.*, **117**, 7132 (2017)
6. W.J.Hyun, C.M.Thomas, M.C.Hersam. *Adv. Energy Mater.*, **10**, 1 (2020)
7. O.Nordness, J.F.Brennecke. *Chem. Rev.*, **120**, 12873 (2020)
8. Y.-L.L.Wang, B.Li, S.Sarman, F.Mocci, Z.Y.Lu, J.Yuan, A.Laaksonen, M.D.Fayer. *Chem. Rev.*, **120**, 5798 (2020)
9. S.Bai, P.Da, C.Li, Z.Wang, Z.Yuan, F.Fu, M.Kawecki, X.Liu, N.Sakai, J.T.W.Wang, S.Huettner, S.Buecheler, M.Fahlman, F.Gao, H.J.Snaith. *Nature*, **571**, 245 (2019)
10. D.Bedrov, J.P.Piquemal, O.Borodin, A.D.MacKerell, B.Roux, C.Schröder. *Chem. Rev.*, **119**, 7940 (2019)
11. K.Dong, X.Liu, H.Dong, X.Zhang, S.Zhang. *Chem. Rev.*, **117**, 6636 (2017)
12. R.Hayes, G.G.G.Warr, R.Atkin. *Chem. Rev.*, **115**, 6357 (2015)
13. H.Weingärtner. *Angew. Chem., Int. Ed.*, **47**, 654 (2008)
14. X.Rao, J.Zhang, J.Zheng, Z.Song, S.Shang. *RSC Adv.*, **4**, 25334 (2014)
15. K.Goossens, K.Lava, C.W.Bielawski, K.Binnemans. *Chem. Rev.*, **116**, 4643 (2016)
16. X.Wang, M.Sternberg, F.T.U.Kohler, B.U.Melcher, P.Wasserscheid, K.Meyer. *RSC Adv.*, **4**, 12476 (2014)
17. T.Ichikawa, T.Kato, H.Ohno. *Chem. Commun.*, **55**, 8205 (2019)
18. R.Tao, E.Gurung, M.M.Cetin, M.F.Mayer, E.L.Quitevis, S.L.Simon. *Thermochim. Acta*, **654**, 121 (2017)
19. Y.Ishikawa, T.Takekiyo, Y.Yoshimura. *J. Mol. Liq.*, **272**, 1019 (2018)
20. H.Abe. *J. Mol. Liq.*, **332**, 115189 (2021)
21. K.Binnemans. *Chem. Rev. (Washington, DC, United States)*, **105**, 4148 (2005)
22. K.Takashi. *Science*, **295**, 2414 (2002)
23. M.Armand, F.Endres, D.R.MacFarlane, H.Ohno, B.Scrosati. *Nat. Mater.*, **8**, 621 (2009)
24. H.Matsumoto, T.Matsuda, T.Tsuda, R.Hagiwara, Y.Ito, Y.Miyazaki. *Chem. Lett.*, 26 (2001)

25. W.Kubo, T.Kitamura, K.Hanabusa, Y.Wada, S.Yanagida. *Chem. Commun.*, **4**, 374 (2002)
26. A.Riisager, R.Fehrmann, M.Haumann, P.Wasserscheid. *Top. Catal.*, **40**, 91 (2006)
27. H.P.Steinrück, J.Libuda, P.Wasserscheid, T.Cremer, C.Kolbeck, M.Laurin, F.Maier, M.Sobota, P.S.Schulz, M.Stark. *Adv. Mater.*, **23**, 2571 (2011)
28. J.Kocher, F.Gumy, A.S.Chauvin, J.C.G.G.Bünzli. *J. Mater. Chem.*, **17**, 654 (2007)
29. Y.Yoshida, G.G.Saito. *Phys. Chem. Chem. Phys.*, **12**, 1675 (2010)
30. J.P.Hallett, T.Welton. *Chem. Rev.*, **111**, 3508 (2011)
31. F.van Rantwijk, R.A.Sheldon. *Chem. Rev.*, **107**, 2757 (2007)
32. V.I.Pârvulescu, C.Hardacre. *Chem. Rev.*, **107**, 2615 (2007)
33. B.V Romanovsky, I.G.G.Tarkhanova. *Russ. Chem. Rev.*, **86**, 444 (2017)
34. H.Sillescu. *J. Non. Cryst. Solids*, **243**, 81 (1999)
35. A.Wisitsorasak, P.G.G.Wolynes. *J. Phys. Chem. B*, **118**, 7835 (2014)
36. K.Grzybowska, A.Grzybowski, Z.Wojnarowska, J.Knapik, M.Paluch. *Sci. Rep.*, **5**, 16876 (2015)
37. E.W.Castner, C.J.Margulis, M.Maroncelli, J.F.Wishart. *Annu. Rev. Phys. Chem.*, **62**, 85 (2011)
38. A.Triolo, O.Russina, H.-J.Bleif, E.Di Cola. *J. Phys. Chem. B*, **111**, 4641 (2007)
39. M.D.Ediger. *Annu. Rev. Phys. Chem.*, **51**, 99 (2000)
40. O.Russina, A.Triolo, Y.Aihara, M.T.F.Telling, H.Grimm. *Macromolecules*, **37**, 8653 (2004)
41. H.Weingärtner. *Curr. Opin. Colloid Interface Sci.*, **18**, 183 (2013)
42. A.Rivera, A.Brodin, A.Pugachev, E.A.Rössler. *J. Chem. Phys.*, **126**, 114503 (2007)
43. M.Y.Ivanov, M.V.Fedin. *Mendeleev Commun.*, **28**, 565 (2018)
44. J.Lu, F.Yan, J.Texter. *Prog. Polym. Sci.*, **34**, 431 (2009)
45. M.P.Scott, M.Rahman, C.S.Brazel. *Eur. Polym. J.*, **39**, 1947 (2003)
46. L.Li, F.Wang, J.Li, X.Yang, J.You. *Int. J. Hydrogen Energy*, **42**, 12087 (2017)
47. M.A.B.H.Susan, T.Kaneko, A.Noda, M.Watanabe. *J. Am. Chem. Soc.*, **127**, 4976 (2005)
48. M.Rahman, C.S.Brazel. *Polym. Degrad. Stab.*, **91**, 3371 (2006)
49. E.Jónsson. *Energy Storage Mater.*, **25**, 827 (2020)
50. P.Sippel, P.Lunkenheimer, S.Krohns, E.Thoms, A.Loidl. *Sci. Rep.*, **5**, 1 (2015)
51. H.Ohno, M.Yoshizawa, W.Ogihara. *Electrochim. Acta*, **48**, 2079 (2003)
52. A.Guyomard-Lack, P.E.Delannoy, N.Dupré, C.V.Cerclier, B.Humbert, J. Le Bideau. *Phys. Chem. Chem. Phys.*, **16**, 23639 (2014)
53. J.Le Bideau, P.Gaveau, S.Bellayer, M.A.Néouze, A.Vioux. *Phys. Chem. Chem. Phys.*, **9**, 5419 (2007)
54. M.A.Néouze, J.Le Bideau, P.Gaveau, S.Bellayer, A.Vioux. *Chem. Mater.*, **18**, 3931 (2006)
55. H.Ohno, M.Yoshizawa, W.Ogihara. *Electrochim. Acta*, **50**, 255 (2004)
56. T.Echelmeyer, H.W.Meyer, L.Van Wiillen. *Chem. Mater.*, **21**, 2280 (2009)
57. C.A.Angell. *Chem. Rev.*, **90**, 523 (1990)
58. E.D.Zanotto, J.C.Mauro. *J. Non. Cryst. Solids*, **471**, 490 (2017)
59. J.Zhao, E.Ragazzi, G.B.McKenna. *Polymer (Guildf)*, **54**, 7041 (2013)
60. J.Zhao, S.L.Simon, G.B.McKenna. *Nat. Commun.*, **4**, 1 (2013)
61. R.Böhmer, C.A.Angell. *Phys. Rev. B*, **45**, 10091 (1992)
62. L.-M.Wang, C.A.Angell. *J. Chem. Phys.*, **118**, 10353 (2003)
63. O.Yamamuro, Y.Minamimoto, Y.Inamura, S.Hayashi, H.O.Hamaguchi. *Chem. Phys. Lett.*, **423**, 371 (2006)
64. O.Yamamuro, T.Yamada, M.Kofu, M.Nakakoshi, M.Nagao. *J. Chem. Phys.*, **135**, 054508 (2011)
65. A.V.Blokhin, Y.U.Paulechka, A.A.Strechan, G.J. Kabo. *J. Phys. Chem. B*, **112**, 4357 (2008)
66. C.A.Angell. *J. Non. Cryst. Solids*, **131**, 13 (1991)
67. R.Richert, C.A.Angell. *J. Chem. Phys.*, **108**, 9016 (1998)
68. A.P.Sokolov, A.Kisliuk, D.Quitmann, A.Kudlik, E.Rössler. *J. Non. Cryst. Solids*, **172 – 174**, 138 (1994)
69. R.Böhmer, K.L.Ngai, C.A.Angell, D.J. Plazek. *J. Chem. Phys.*, **99**, 4201 (1993)
70. K.Ueno, Z.Zhao, M.Watanabe, C.A.Angell. *J. Phys. Chem. B*, **116**, 63 (2012)
71. Q.Qin, G.B.McKenna. *J. Non. Cryst. Solids*, **352**, 2977 (2006)
72. C.A.Angell, K.L.Ngai, G.B.McKenna, P.F.McMillan, S.W.Martin. *J. Appl. Phys.*, **88**, 3113 (2000)
73. G.G.Adam, J.H.Gibbs. *J. Chem. Phys.*, **43**, 139 (1965)
74. M.H.Cohen, D.Turnbull. *J. Chem. Phys.*, **31**, 1164 (1959)
75. V.V.Brazhkin. *JETP Lett.*, **112**, 745 (2020)
76. C.A.Angell. *J. Non. Cryst. Solids*, **73**, 1 (1985)
77. M.K.Mapes, S.F.Swallen, M.D.Ediger. *J. Phys. Chem. B*, **110**, 507 (2006)
78. S.F.Swallen, P.A.Bonvallet, R.J. McMahon, M.D.Ediger. *Phys. Rev. Lett.*, **90**, 4 (2003)
79. A.P.Sokolov, K.S.Schweizer. *Phys. Rev. Lett.*, **102**, 1 (2009)
80. M.D.Ediger, P.Harrowell, L.Yu. *J. Chem. Phys.*, **128**, 034709 (2008)
81. P.Griffin, A.L.Agapov, A.Kisliuk, X.-G.G.Sun, S.Dai, V.N.Novikov, A.P.Sokolov. *J. Chem. Phys.*, **135**, 114509 (2011)
82. W.Xu, E.I.Cooper, C.A.Angell. *J. Phys. Chem. B*, **107**, 6170 (2003)
83. J.R.Sangoro, C.Iacob, A.Serghei, C.Friedrich, F.Kremer. *Phys. Chem. Chem. Phys.*, **11**, 913 (2009)
84. E.Donth. *J. Non. Cryst. Solids*, **53**, 325 (1982)
85. E.Donth, H.Huth, M.Beiner. *J. Phys. Condens. Matter*, **13**, L451 (2001)
86. G.G.Biroli, J.P.Garrahan. *J. Chem. Phys.*, **138**, 12A301 (2013)
87. Q.Zheng, Y.Zhang, M.Montazerian, O.Gulbiten, J.C.Mauro, E.D.Zanotto, Y.Yue. *Chem. Rev.*, **119**, 7848 (2019)
88. L.-M.Wang, C.A.Angell, R.Richert. *J. Chem. Phys.*, **125**, 074505 (2006)
89. C.A.Angell. *Chem. Rev.*, **102**, 2627 (2002)
90. J.C.Lassègues, J.Grondin, R.Holomb, P.Johansson. *J. Raman Spectrosc.*, **38**, 551 (2007)
91. I.M.Kalogeras, H.E.Hagg Lobland. *J. Mater. Educ.*, **34**, 69 (2012)
92. S.Zhang, N.Sun, X.He, X.Lu, X.Zhang. *J. Phys. Chem. Ref. Data*, **35**, 1475 (2006)
93. S.M.Urahata, M.C.C.C.Ribeiro. *J. Chem. Phys.*, **120**, 1855 (2004)
94. J.Leys, M.Wübbenhorst, C.Preethy Menon, R.Rajesh, J.Thoen, C.Glorieux, P.Nockemann, B.Thijs, K.Binnemans, S.Longuemart. *J. Chem. Phys.*, **128**, 1 (2008)
95. C.P.Fredlake, J.M.Crosthwaite, D.G.Hert, S.N.V.K.Aki, J.F.Brennecke. *J. Chem. Eng. Data*, **49**, 954 (2004)
96. T.Erdmenger, J.Vitz, F.Wiesbrock, U.S.Schubert. *J. Mater. Chem.*, **18**, 5267 (2008)
97. H.J.Kwon, J.A.Seo, T.Iwahashi, Y.Ouchi, D.Kim, H.K.Kim, Y.H.Hwang. *Curr. Appl. Phys.*, **13**, 271 (2013)
98. J.D.Holbrey, K.R.Seddon. *J. Chem. Soc., Dalt. Trans.*, 2133 (1999)
99. C.M.Gordon, J.D.Holbrey, A.R.Kennedy, K.R.Seddon. *J. Mater. Chem.*, **8**, 2627 (1998)
100. A.E.Bradley, C.Hardacre, J.D.Holbrey, S.Johnston, S.E.J.McMath, M.Nieuwenhuyzent. *Chem. Mater.*, **14**, 629 (2002)
101. N.Calvar, E.Gómez, E.A.Macedo, Á.Domínguez. *Thermochim. Acta*, **565**, 178 (2013)
102. I.Bandrés, F.M.Royo, I.Gascón, M.Castro, C.Lafuente. *J. Phys. Chem. B*, **114**, 3601 (2010)
103. H.Tokuda, K.Hayamizu, K.Ishii, M.A.B.H.Susan, M.Watanabe. *J. Phys. Chem. B*, **108**, 16593 (2004)

104. P.B.P.Serra, F.M.S.Ribeiro, M.A.A.Rocha, M.Fulem, K.Růžička, L.M.N.B.F.Santos. *J. Chem. Thermodyn.*, **100**, 124 (2016)
105. M.C.C.Ribeiro, A.A.H.Pádua, M.F.C.Gomes. *J. Chem. Phys.*, **140**, 244514 (2014)
106. O.Russina, F.Lo Celso, A.Triolo. *Phys. Chem. Chem. Phys.*, **17**, 29496 (2015)
107. Y.Yoshimura, M.Shigemi, M.Takaku, M.Yamamura, T.Takekiyo, H.Abe, N.Hamaya, D.Wakabayashi, K.Nishida, N.Funamori, T.Sato, T.Kikegawa. *J. Phys. Chem. B*, **119**, 8146 (2015)
108. T.Takekiyo, Y.Koyama, M.Shigemi, K.Matsuishi, H.Abe, N.Hamaya, Y.Yoshimura. *Phys. Chem. Chem. Phys.*, **19**, 863 (2017)
109. M.Shigemi, T.Takekiyo, H.Abe, N.Hamaya, Y.Yoshimura. *J. Solution Chem.*, **43**, 1614 (2014)
110. F.Lo Celso, A.Triolo, L.Gontrani, O.Russina. *J. Chem. Phys.*, **148**, 1 (2018)
111. Y.Yoshimura, T.Takekiyo, Y.Koyama, M.Takaku, M.Yamamura, N.Kikuchi, D.Wakabayashi, N.Funamori, K.Matsuishi, H.Abe, N.Hamaya. *Phys. Chem. Chem. Phys.*, **20**, 199 (2017)
112. M.Paluch, S.Hensel-Bielówka, J.Zioło. *J. Chem. Phys.*, **110**, 10978 (1999)
113. M.Paluch, J.Gapinski, A.Patkowski, E.W.Fischer. *J. Chem. Phys.*, **114**, 8048 (2001)
114. A.Martinelli, A.Matic, P.Johansson, P.Jacobsson, L.Börjesson, A.Fernicola, S.Panero, B.Scrosati, H.Ohno. *J. Raman Spectrosc.*, **42**, 522 (2011)
115. F.M.Vitucci, F.Trequattrini, O.Palumbo, J.-B.Brubach, P.Roy, M.A.Navarra, S.Panero, A.Paolone. *J. Phys. Chem. A*, **118**, 8758 (2014)
116. F.Capitani, F.Trequattrini, O.Palumbo, A.Paolone, P.Postorino. *J. Phys. Chem. B*, **120**, 2921 (2016)
117. T.A.Lima, L.F.O.Faria, V.H.Paschoal, M.C.C.Ribeiro. *J. Chem. Phys.*, **148**, 171101 (2018)
118. Y.Yoshimura, T.Takekiyo, Y.Imai, H.Abe. *J. Phys. Chem. C*, **116**, 2097 (2012)
119. F.Capitani, S.Gatto, P.Postorino, O.Palumbo, F.Trequattrini, M.Deutsch, J.B.Brubach, P.Roy, A.Paolone. *J. Phys. Chem. B*, **120**, 1312 (2016)
120. M.Herstedt, M.Smirnov, P.Johansson, M.Chami, J.Grondin, L.Servant, J.C.Lassègues. *J. Raman Spectrosc.*, **36**, 762 (2005)
121. O.Palumbo, F.Trequattrini, F.M.Vitucci, A.Paolone. *J. Phys. Chem. B*, **119**, 12905 (2015)
122. K.Fujii, T.Fujimori, T.Takamuku, R.Kanzaki, Y.Umebayashi, S.I.Ishiguro. *J. Phys. Chem. B*, **110**, 8179 (2006)
123. F.M.Vitucci, O.Palumbo, F.Trequattrini, J.-B.Brubach, P.Roy, I.Meschini, F.Croce, A.Paolone. *J. Chem. Phys.*, **143**, 094707 (2015)
124. L.Su, L.Li, Y.Hu, C.Yuan, C.Shao, S.Hong. *J. Chem. Phys.*, **130**, 4 (2009)
125. T.Endo, T.Kato, K.I.Tozaki, K.Nishikawa. *J. Phys. Chem. B*, **114**, 407 (2010)
126. O.Russina, B.Fazio, C.Schmidt, A.Triolo. *Phys. Chem. Chem. Phys.*, **13**, 12067 (2011)
127. H.Abe, T.Takekiyo, N.Hatano, M.Shigemi, N.Hamaya, Y.Yoshimura. *J. Phys. Chem. B*, **118**, 1138 (2014)
128. I.Avramov. *J. Non. Cryst. Solids*, **351**, 3163 (2005)
129. Z.Wojnarowska, M.Paluch, A.Grzybowski, K.Adrjanowicz, K.Grzybowska, K.Kaminski, P.Wlodarczyk, J.Pionteck. *J. Chem. Phys.*, **131**, 104505 (2009)
130. S.P.Andersson, O.Andersson. *Macromolecules*, **31**, 2999 (1998)
131. H.Li, Z.Wang, L.Chen, J.Wu, H.Huang, K.Yang, Y.Wang, L.Su, G.G.Yang. *J. Phys. Chem. B*, **119**, 14245 (2015)
132. L.F.O.Faria, M.C.C.Ribeiro. *J. Phys. Chem. B*, **119**, 14315 (2015)
133. Y.Yoshimura, H.Abe, Y.Imai, T.Takekiyo, N.Hamaya. *J. Phys. Chem. B*, **117**, 3264 (2013)
134. J.F.Mammone, S.K.Sharma, M.Nicol. *J. Phys. Chem.*, **84**, 3130 (1980)
135. W.Xu, L.-M.M.Wang, R.A.Nieman, C.A.Angell. *J. Phys. Chem. B*, **107**, 11749 (2003)
136. J.Sun, M.Forsyth, D.R.MacFarlane. *J. Phys. Chem. B*, **102**, 8858 (1998)
137. S.Zhang, J.Zhang, Y.Zhang, Y.Deng. *Chem. Rev.*, **117**, 6755 (2017)
138. L.Li, J.Groenewold, S.J.Picken. *Chem. Mater.*, **17**, 250 (2005)
139. X.Chen, Q.Li, J.Zhao, L.Qiu, Y.Zhang, B.Sun, F.Yan. *J. Power Sources*, **207**, 216 (2012)
140. G.G.Wang, C.Yan, J.Zhang, S.Hou, W.Zhang. *J. Power Sources*, **345**, 131 (2017)
141. C.P.Lee, K.C.Ho. *Eur. Polym. J.*, **108**, 420 (2018)
142. Y.L.Verma, M.P.Singh, R.K.Singh. *Mater. Lett.*, **86**, 73 (2012)
143. C.Espejo, F.J.Carrion, D.Martinez, M.D.Bermudez. *Tribol. Lett.*, **50**, 127 (2013)
144. F.Taherkhani, B.Minofar. *J. Phys. Chem. C*, **121**, 15493 (2017)
145. F.J.Carrión, J.Sanes, M.D.Bermúdez, A.Arribas. *Tribol. Lett.*, **41**, 199 (2011)
146. M.P.Singh, R.K.Singh, S.Chandra. *J. Phys. Chem. B*, **115**, 7505 (2011)
147. R.Göbel, P.Hesemann, J.Weber, E.Möller, A.Friedrich, S.Beuermann, A.Taubert. *Phys. Chem. Chem. Phys.*, **11**, 3653 (2009)
148. G.G.Kritikos, N.Vergadou, I.G.G.Economou. *J. Phys. Chem. C*, **120**, 1013 (2016)
149. M.Y.Ivanov, A.S.Poryvaev, D.M.Polyukhov, S.A.Prikhod ko, N.Y.Adonin, M.V.Fedin. *Nanoscale*, **12**, 23480 (2020)
150. C.Alba-Simionesco, B.Coasne, G.G.Dosseh, G.G.Dudziak, K.E.Gubbins, R.Radhakrishnan, M.Sliwinska-Bartkowiak. *J. Phys. Condens. Matter*, **18**, R15 (2006)
151. G.G.Dosseh, Y.Xia, C.Alba-Simionesco. *J. Phys. Chem. B*, **107**, 6445 (2003)
152. Y.Xia, G.G.Dosseh, D.Morineau, C.Alba-Simionesco. *J. Phys. Chem. B*, **110**, 19735 (2006)
153. D.Morineau, Y.Xia, C.Alba-Simionesco. *J. Chem. Phys.*, **117**, 8966 (2002)
154. Y.Yoshimura, H.Kimura, C.Okamoto, T.Miyashita, Y.Imai, H.Abe. *J. Chem. Thermodyn.*, **43**, 410 (2011)
155. L.P.N.N.Rebelo, V.Najdanovic-Visak, Z.P.Visak, M.Nunes da Ponte, J.Szydlowski, C.A.Cerdeiriña, J.Troncoso, L.Romaní, J.M.S.S.S.Esperança, H.J.R.Guedes, H.C.de Sousa. *Green Chem.*, **6**, 369 (2004)
156. Y.Imai, H.Abe, T.Miyashita, T.Goto, H.Matsumoto, Y.Yoshimura. *Chem. Phys. Lett.*, **486**, 37 (2010)
157. A.Inaba, O.Andersson. *Thermochim. Acta*, **461**, 44 (2007)
158. Y.Yoshimura, T.Goto, H.Abe, Y.Imai. *J. Phys. Chem. B*, **113**, 8091 (2009)
159. M.T.Clough, C.R.Crick, J.Gräsvik, P.A.Hunt, H.Niedermeyer, T.Welton, O.P.Whitaker. *Chem. Sci.*, **6**, 1101 (2015)
160. J.Scheers, J.Pitawala, F.Thebault, J.K.Kim, J.H.Ahn, A.Matic, P.Johansson, P.Jacobsson. *Phys. Chem. Chem. Phys.*, **13**, 14953 (2011)
161. I.Siretanu, H.Saadaoui, J.P.Chapel, C.Drummond. *Macromolecules*, **48**, 2787 (2015)
162. L.Alzate-Vargas, N.Onofrio, A.Strachan. *Macromolecules*, **53**, 9375 (2020)
163. Y.Ji, R.Shi, Y.Wang, G.G.Saielli. *J. Phys. Chem. B*, **117**, 1104 (2013)
164. Y.Wang, W.G.Noid, P.Liu, G.A.Voth. *Phys. Chem. Chem. Phys.*, **11**, 2002 (2009)
165. O.Russina, A.Triolo, L.Gontrani, R.Caminiti. *J. Phys. Chem. Lett.*, **3**, 27 (2012)

166. S.Kashin, K.I.Galkin, E.A.Khokhlova, V.P.Ananikov. *Angew. Chem., Int. Ed.*, **55**, 2161 (2016)
167. H.Gao, J.Li, B.Han, W.Chen, J.Zhang, R.Zhang, D.Yan. *Phys. Chem. Chem. Phys.*, **6**, 2914 (2004)
168. P.Madhavan, R.Sougrat, A.R.Behzad, K.V.Peinemann, S.P.Nunes. *J. Memb. Sci.*, **492**, 568 (2015)
169. A.Triolo, O.Russina, V.Arrighi, F.Juranyi, S.Janssen, C.M.Gordon. *J. Chem. Phys.*, **119**, 8549 (2003)
170. A.Triolo, O.Russina, C.Hardacre, M.Nieuwenhuyzen, M.A.Gonzalez, H.Grimm. *J. Phys. Chem. B*, **109**, 22061 (2005)
171. A.Triolo, A.Mandanici, O.Russina, V.Rodriguez-Mora, M.Cutroni, C.Hardacre, M.Nieuwenhuyzen, H.-J.J.Bleif, L.Keller, M.A.Ramos. *J. Phys. Chem. B*, **110**, 21357 (2006)
172. G.J.Kabo, A.V.Blokhin, Y.U.Paulechka, A.G.G.Kabo, M.P.Shymanovich, J.W.Magee. *J. Chem. Eng. Data*, **49**, 453 (2004)
173. C.G.G.Hanke, S.L.Price, R.M.Lynden-Bell. *Mol. Phys.*, **99**, 801 (2001)
174. C.Hardacre, S.E.J.McMath, M.Nieuwenhuyzen, D.T.Bowron, A.K.Soper. *J. Phys. Condens. Matter*, **15**, S159 (2003)
175. A.Rivera, E.A.Rössler. *Phys. Rev. B: Condens. Matter Mater. Phys.*, **73**, 1 (2006)
176. N.Ito, R.Richert. *J. Phys. Chem. B*, **111**, 5016 (2007)
177. H.Cang, J.Li, M.D.Fayer. *J. Chem. Phys.*, **119**, 13017 (2003)
178. J. Li, I.Wang, K.Fruchey, M.D.Fayer. *J. Phys. Chem. A*, **110**, 10384 (2006)
179. W.Huang, R.Richert. *J. Chem. Phys.*, **131**, 184501 (2009)
180. P.J. Griffin, A.L.Agapov, A.P.Sokolov. *Phys. Rev. E*, **86**, 021508 (2012)
181. V.V.Matveev, D.A.Markelov, E.A.Brui, V.I.Chizhik, P.Ingman, E.Lähderanta. *Phys. Chem. Chem. Phys.*, **16**, 10480 (2014)
182. J.H.Antony, D.Mertens, A.Dölle, P.Wasserscheid, W.R.Carper. *ChemPhysChem*, **4**, 588 (2003)
183. K.Hayamizu, S.Tsuzuki, S.Seki. *J. Phys. Chem. A*, **112**, 12027 (2008)
184. H.Zhu, L.A.O Dell. *Chem. Commun.*, **57**, 5609 (2021)
185. T.Endo, S.Sen. *J. Phys. Chem. B*, **118**, 14888 (2014)
186. N.Bloembergen, E.M.Purcell, R.V.Pound. *Phys. Rev.*, **73**, 679 (1948)
187. A.E.Khudozhitkov, J.Neumann, T.Niemann, D.Zaitsau, P.Stange, D.Paschek, A.G.G.Stepanov, D.I.Kolokolov, R.Ludwig. *Angew. Chemie - Int. Ed.*, **58**, 17863 (2019)
188. A.Strate, J.Neumann, T.Niemann, P.Stange, A.E.Khudozhitkov, A.G.G.Stepanov, D.Paschek, D.I.Kolokolov, R.Ludwig. *Phys. Chem. Chem. Phys.*, **22**, 6861 (2020)
189. A.E.Khudozhitkov, T.Niemann, P.Stange, M.Donoshita, A.G.G.Stepanov, H.Kitagawa, D.I.Kolokolov, R.Ludwig. *J. Phys. Chem. Lett.*, **11**, 6000 (2020)
190. P.S.Gill, S.R.Sauerbrunn, M.Reading. *J. Therm. Anal.*, **40**, 931 (1993)
191. C.Dalle-Ferrier, C.Thibierge, C.Alba-Simionesco, L.Berthier, G.G.Biroli, J.-P.Bouchaud, F.Ladieu, D.L Hôte, G.G.Tarjus. *Phys. Rev. E*, **76**, 041510 (2007)
192. E.Hempel, G.G.Hempel, A.Hensel, C.Schick, E.Donth. *J. Phys. Chem. B*, **104**, 2460 (2000)
193. J.Wang, Y.Tian, Y.Zhao, K.Zhuo. *Green Chem.*, **5**, 618 (2003)
194. J.A.Widegren, A.Laesecke, J.W.Magee. *Chem. Commun.*, 1610 (2005)
195. V.Najdanovic-Visak, J.M.S.S.Esperança, L.P.N.Rebelo, M.N.Da Ponte, H.J.R.Guedes, K.R.Seddon, H.C.De Sousa, J.Szydlowski. *J. Phys. Chem. B*, **107**, 12797 (2003)
196. L.Zhang, Z.Xu, Y.Wang, H.Li. *J. Phys. Chem. B*, **112**, 6411 (2008)
197. M.Y.Ivanov, O.A.Krumkacheva, S.A.Dzuba, M.V.Fedin. *Phys. Chem. Chem. Phys.*, **19**, 26158 (2017)
198. M.Y.Ivanov, S.A.Prikhod ko, N.Y.Adonin, I.A.Kirilyuk, S.V.Adichtchev, N.V.Surovtsev, S.A.Dzuba, M.V.Fedin. *J. Phys. Chem. Lett.*, **9**, 4607 (2018)
199. M.Y.Ivanov, S.A.Prikhod ko, N.Y.Adonin, M.V.Fedin. *J. Phys. Chem. B*, **123**, 9956 (2019)
200. O.D.Bakulina, M.Y.Ivanov, S.A.Prikhod ko, S.Pylaeva, I.V.Zaytseva, N.V.Surovtsev, N.Y.Adonin, M.V.Fedin. *Nanoscale*, **12**, 19982 (2020)
201. S.V.Paschenko, Y.V.Toropov, S.A.Dzuba, Y.D.Tsvetkov, A.K.Vorobiev. *J. Chem. Phys.*, **110**, 8150 (1999)
202. S.A.Dzuba, E.P.Kirilina, E.S.Salnikov. *J. Chem. Phys.*, **125**, 054502 (2006)
203. D.A.Erilov, R.Bartucci, R.Guzzi, D.Marsh, S.A.Dzuba, L.Sportelli. *Biophys. J.*, **87**, 3873 (2004)
204. D.A.Erilov, R.Bartucci, R.Guzzi, D.Marsh, S.A.Dzuba, L.Sportelli. *J. Phys. Chem. B*, **108**, 4501 (2004)
205. N.P.Isaev, M.V.Fedin, S.A.Dzuba. *Appl. Magn. Reson.*, **44**, 133 (2013)
206. V.N.Syryamina, S.A.Dzuba. *J. Phys. Chem. B*, **121**, 1026 (2017)
207. L.V.Kulik, L.L.Rapatsky, A.V.Pivtsov, N.V.Surovtsev, S.V.Adichtchev, I.A.Grigor'ev, S.A.Dzuba. *J. Chem. Phys.*, **131**, 064505 (2009)
208. N.V.Surovtsev, N.V.Ivanisenko, K.Y.Kirillov, S.A.Dzuba. *J. Phys. Chem. B*, **116**, 8139 (2012)
209. N.V.Surovtsev, S.A.Dzuba. *J. Chem. Phys.*, **140**, 235103 (2014)
210. K.Wood, M.Plazanet, F.Gabel, B.Kessler, D.Oesterhelt, D.J.Tobias, G.G.Zaccai, M.Weik. *Proc. Natl. Acad. Sci. USA*, **104**, 18049 (2007)
211. K.Wood, M.Plazanet, F.Gabel, B.Kessler, D.Oesterhelt, G.G.Zaccai, M.Weik. *Eur. Biophys. J.*, **37**, 619 (2008)
212. A.Frölich, F.Gabel, M.Jasnin, U.Lehnert, D.Oesterhelt, A.M.Stadler, M.Tehei, M.Weik, K.Wood, G.G.Zaccai. *Faraday Discuss.*, **141**, 117 (2009)
213. D.J.Tobias, N.Sengupta, M.Tarek. *Faraday Discuss.*, **141**, 99 (2009)
214. A.A.Kuzhelev, O.A.Krumkacheva, M.Y.Ivanov, S.A.Prikhod ko, N.Y.Adonin, V.M.Tormyshev, M.K.Bowman, M.V.Fedin, *E.G*.G.Bagryanskaya. *J. Phys. Chem. B*, **122**, 8624 (2018)
215. A.Zecevic, G.R.Eaton, S.S.Eaton, M.Lindgren. *Mol. Phys.*, **95**, 1255 (1998)
216. L.Andreozzi, A.Di Schino, M.Giordano, D.Leporini. *Europhys. Lett.*, **38**, 669 (1997)
217. R.Owenius, G.R.Eaton, S.S.Eaton. *J. Magn. Reson.*, **172**, 168 (2005)
218. I.A.Kirilyuk, Y.F.Polienko, O.A.Krumkacheva, R.K.Strizhakov, Y.V.Gatilov, I.A.Grigor'ev, E.G.G.Bagryanskaya. *J. Org. Chem.*, **77**, 8016 (2012)
219. J.Habasaki, K.L.Ngai. *J. Phys. Soc. Jpn.*, **79**, 145 (2010)
220. J.Habasaki, K.L.Ngai. *J. Non. Cryst. Solids*, **357**, 446 (2011)
221. J.Habasaki, K.L.Ngai. *Anal. Sci.*, **24**, 1321 (2008)
222. J.Habasaki, K.L.Ngai. *J. Chem. Phys.*, **129**, 194501 (2008)
223. J.Habasaki, K.L.Ngai. *J. Chem. Phys.*, **142**, 164501 (2015)
224. Y.F.Hu, X.M.Zhang, J.G.G.Qi, L.Y.Yin. *J. Chem. Phys.*, **143**, 1 (2015)
225. A.Rodríguez-Rivas, J.M.Romero-Enrique, L.F.Rull. *Mol. Phys.*, **117**, 3941 (2019)
226. T.Pal, M.Vogel. *ChemPhysChem*, **18**, 2233 (2017)
227. N.Jafari, B.Arab, N.Zekri, R.Fareghi-Alamdari. *Propellants, Explos. Pyrotech.*, **45**, 615 (2020)
228. K.Kothari, V.Ragoonanan, R.Suryanarayanan. *Mol. Pharm.*, **11**, 3048 (2014)
229. M.Mehta, V.Ragoonanan, G.B.McKenna, R.Suryanarayanan. *Mol. Pharm.*, **13**, 1267 (2016)
230. K.Adrjanowicz, D.Zakowiecki, K.Kaminski, L.Hawelek, K.Grzybowska, M.Tarnacka, M.Paluch, K.Cal. *Mol. Pharm.*, **9**, 1748 (2012)

231. R.Ferraz, L.C.Branco, C.Prudêncio, J.P.Noronha, Ž.Petrovski. *ChemMedChem*, **6**, 975 (2011)
232. W.L.Hough, M.Smiglak, H.Rodríguez, R.P.Swatloski, S.K.Spear, D.T.Daly, J. Pernak, J.E.Grisel, R.D.Carliss, M.D.Soutullo, J.H.Davis, R.D.Rogers. *New J. Chem.*, **31**, 1429 (2007)
233. W.L.Hough, R.D.Rogers. *Bull. Chem. Soc. Jpn.*, **80**, 2262 (2007)
234. J.Stoimenovski, D.R.MacFarlane, K.Bica, R.D.Rogers. *Pharm. Res.*, **27**, 521 (2010)
235. J.Stoimenovski, P.M.Dean, E.I.Izgorodina, D.R.MacFarlane. *Faraday Discuss.*, **154**, 335 (2012)
236. R.F.M.Frade, A.A.Rosatella, C.S.Marques, L.C.Branco, P.S.Kulkarni, N.M.M.Mateus, C.A.M.Afonso, C.M.M.Duarte. *Green Chem.*, **11**, 1660 (2009)
237. M.T.Viciosa, G.G.Santos, A.Costa, F.Danède, L.C.Branco, N.Jordão, N.T.Correia, M.Dionísio. *Phys. Chem. Chem. Phys.*, **17**, 24108 (2015)
238. H.P.Diogo, J.J.Moura Ramos. *Soft Mater.*, **12**, 125 (2014)
239. Z.Wojnarowska, C.M.Roland, K.Kolodziejczyk, A.Swiety-Pospiech, K.Grzybowska, M.Paluch. *J. Phys. Chem. Lett.*, **3**, 1238 (2012)
240. Z.Wojnarowska, C.M.Roland, A.Swiety-Pospiech, K.Grzybowska, M.Paluch. *Phys. Rev. Lett.*, **108**, 1 (2012)
241. Z.Wojnarowska, K.Kołodziejczyk, K.J.Paluch, L.Tajber, K.Grzybowska, K.L.Ngai, M.Paluch. *Phys. Chem. Chem. Phys.*, **15**, 9205 (2013)
242. C.A.Angell. *J. Phys. Chem. Solids*, **49**, 863 (1988)
243. M.D.Ediger, C.A.Angell, S.R.Nagel. *J. Phys. Chem.*, **100**, 13200 (1996)
244. C.A.Angell. *Science*, **267**, 1924 (1995)
245. M.Jackson, H.H.Mantsch. *Biochim. Biophys. Acta — Protein Struct. Mol. Enzymol.*, **1078**, 231 (1991)
246. G.M.Fahy. *Cryobiology*, **23**, 1 (1986)
247. Y.Yoshimura, T.Takekiyo, T.Mori. *Chem. Phys. Lett.*, **664**, 44 (2016)
248. T.Takekiyo, E.Yamaguchi, K.Yoshida, M.Kato, T.Yamaguchi, Y.Yoshimura. *J. Phys. Chem. B*, **119**, 6536 (2015)
249. Y.Shu, M.Liu, S.Chen, X.Chen, J.Wang. *J. Phys. Chem. B*, **115**, 12306 (2011)
250. T.Takekiyo, K.Yamazaki, E.Yamaguchi, H.Abe, Y.Yoshimura. *J. Phys. Chem. B*, **116**, 11092 (2012)
251. T.Takekiyo, E.Yamaguchi, H.Abe, Y.Yoshimura. *ACS Sustain. Chem. Eng.*, **4**, 422 (2016)
252. T.Takekiyo, Y.Ishikawa, Y.Yoshimura. *J. Phys. Chem. B*, **121**, 7614 (2017)
253. T.Takekiyo, K.Yoshida, Y.Funahashi, S.Nagata, H.Abe, T.Yamaguchi, Y.Yoshimura. *J. Mol. Liq.*, **243**, 584 (2017)
254. T.Takekiyo, Y.Koyama, K.Yamazaki, H.Abe, Y.Yoshimura. *J. Phys. Chem. B*, **117**, 10142 (2013)
255. H.Ohno, K.Fukumoto. *Acc. Chem. Res.*, **40**, 1122 (2007)
256. P.Kubisa. *Prog. Polym. Sci.*, **29**, 3 (2004)
257. P.Kubisa. *Prog. Polym. Sci.*, **34**, 1333 (2009)
258. T.Biedron, P.Kubisa. *Polym. Int.*, **52**, 1584 (2003)
259. R.Vijayaraghavan, D.R.MacFarlane. *Chem. Commun.*, **4**, 700 (2004)
260. J.M.Pringle, J.Efthimiadis, P.C.Howlett, J.Efthimiadis, D.R.MacFarlane, A.B.Chaplin, S.B.Hall, D.L.Officer, G.G.G.Wallace, M.Forsyth. *Polymer (Guildf.)*, **45**, 1447 (2004)
261. V.Strehmel, S.Berdzinski, L.Ehrentraut, C.Faßbender, J.Horst, E.Leeb, J.Liepert, M.P.Ruby, V.Senkowski, P.Straßburg, A.Wenda, C.Strehmel. *Prog. Org. Coatings*, **89**, 297 (2015)
262. Z.Wojnarowska, J.Knapik, M.Díaz, A.Ortiz, I.Ortiz, M.Paluch. *Macromolecules*, **47**, 4056 (2014)
263. V.Strehmel, V.Senkowski. *J. Polym. Sci. Part A Polym. Chem.*, **53**, 2849 (2015)
264. M.P.Scott, C.S.Brazel, M.G.G.Benton, J.W.Mays, J.D.Holbrey, R.D.Rogers. *Chem. Commun.*, **2**, 1370 (2002)
265. M.Lee, U.H.Choi, R.H.Colby, H.W.Gibson. *Chem. Mater.*, **22**, 5814 (2010)
266. N.Kamaya, K.Homma, Y.Yamakawa, M.Hirayama, R.Kanno, M.Yonemura, T.Kamiyama, Y.Kato, S.Hama, K.Kawamoto, A.Mitsui. *Nat. Mater.*, **10**, 682 (2011)
267. X.Wang, B.Liu, Q.Wang, W.Song, X.Hou, D.Chen, Y.B.Cheng, G.G.Shen. *Adv. Mater.*, **25**, 1479 (2013)
268. Z.Niu, H.Dong, B.Zhu, J.Li, H.H.Hng, W.Zhou, X.Chen, S.Xie. *Adv. Mater.*, **25**, 1058 (2013)
269. C.Zhong, Y.Deng, W.Hu, J.Qiao, L.Zhang, J.Zhang. *Chem. Soc. Rev.*, **44**, 7484 (2015)
270. N.P.Tarasova, Y.V Smetannikov, A.A.Zanin. *Russ. Chem. Rev.*, **79**, 463 (2010)
271. A.Hagfeldt, G.G.Boschloo, L.Sun, L.Kloo, H.Pettersson. *Chem. Rev.*, **110**, 6595 (2010)
272. T.Ueki, M.Watanabe. *Macromolecules*, **41**, 3739 (2008)
273. M.Li, L.Yang, S.Fang, S.Dong, S.I.Hirano, K.Tachibana. *Polym. Int.*, **61**, 259 (2012)
274. S.Isikli, K.M.Ryan. *Curr. Opin. Electrochem.*, **21**, 188 (2020)
275. D.R.Macfarlane, N.Tachikawa, M.Forsyth, J.M.Pringle, P.C.Howlett, G.D.Elliott, J.H.Davis, M.Watanabe, P.Simon, C.A.Angell. *Energy Environ. Sci.*, **7**, 232 (2014)
276. M.Hirao, H.Sugimoto, H.Ohno. *J. Electrochem. Soc.*, **147**, 4168 (2000)
277. H.C.Chang, C.Y.Chang, J.C.Su, W.C.Chu, J.C.Jiang, H.L.Sheng. *Int. J. Mol. Sci.*, **7**, 417 (2006)
278. A.Hayashi, H.Morishima, K.Tadanaga, M.Tatsumisago. *Solid State Ionics*, **192**, 126 (2011)
279. Q.Ma, H.Zhang, C.Zhou, L.Zheng, P.Cheng, J.Nie, W.Feng, Y.S.Hu, H.Li, X.Huang, L.Chen, M.Armand, Z.Zhou. *Angew. Chem., Int. Ed.*, **55**, 2521 (2016)
280. M.Yoshizawa, A.Narita, H.Ohno. *Aust. J. Chem.*, **57**, 139 (2004)
281. S.Seki, M.A.B.H.Susan, T.Kaneko, H.Tokuda, A.Noda, M.Watanabe. *J. Phys. Chem. B*, **109**, 3886 (2005)
282. Y.Lu, S.S.Moganty, J.L.Schaefer, L.A.Archer. *J. Mater. Chem.*, **22**, 4066 (2012)
283. Z.Wojnarowska, Y.Wang, J.Pionteck, K.Grzybowska, A.P.Sokolov, M.Paluch. *Phys. Rev. Lett.*, **111**, 1 (2013)
284. K.Nakamura, K.Fukao, T.Inoue. *Macromolecules*, **45**, 3850 (2012)
285. K.Nakamura, K.Fukao. *Polymer (Guildf).*, **54**, 3306 (2013)
286. U.H.Choi, Y.Ye, D.Salas De La Cruz, W.Liu, K.I.Winey, Y.A.Elabd, J.Runt, R.H.Colby. *Macromolecules*, **47**, 777 (2014)